

ADVANCES IN VERIFICATION, VALIDATION, AND UNCERTAINTY QUANTIFICATION FOR COMPUTATIONAL MECHANICS

Brian A. Freno

Verification, Validation, and Uncertainty Quantification
Sandia National Laboratories

General Atomics
September 17, 2025

Biography: Brian Freno

Education: BS, MS, PhD in Aerospace Engineering at Texas A&M University

Work Experience:

Oct. 2015 – Present	Sandia National Laboratories
Jun. 2014 – Sep. 2015	Halliburton
Summers 2012 & 2013	NASA Marshall Space Flight Center
Summers 2007 & 2008	Lockheed Martin Missiles and Fire Control
Summers 2005 & 2006	Standard Aero

Research Areas: reduced-order modeling, code verification, machine learning, computational fluid dynamics, and computational electromagnetics

Publications: primary author of several journal articles and one patent

Service:

- Associate fellow of AIAA, member of ASME & SIAM
- Associate editor for the ASME Journal of VVUQ
- Committees: AIAA Fluid Dynamics, ASME VVUQ for CFD/Heat Transfer
- Adjunct professor in Texas A&M Department of Aerospace Engineering
- Conference session organizer, program & journal reviewer, mentor, recruiter

MACHINE-LEARNING ERROR MODELS FOR APPROXIMATE SOLUTIONS TO PARAMETERIZED SYSTEMS OF NONLINEAR EQUATIONS

Brian A. Freno
Kevin T. Carlberg
Sandia National Laboratories

Motivation

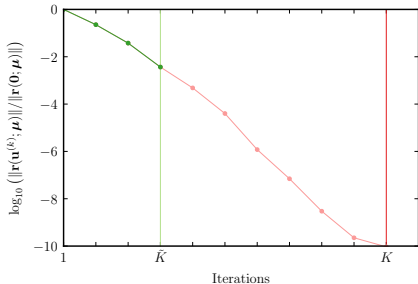
- Many-query problems can impose a formidable computational burden
- **Solution approximations** can exchange fidelity for speed
- Need to quantify the error

Solution Approximations

- **Inexact solutions:** When solving nonlinear equations, prematurely terminate iterations
- **Lower-fidelity models:** Neglect physical phenomena, coarsen the mesh, or use lower-order finite differences or elements
- **Reduced-order models:** Approximate solution with a linear combination of $m_u \ll N_u$ basis functions

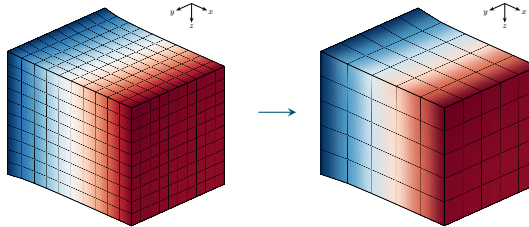
Solution Approximations

- **Inexact solutions:** When solving nonlinear equations, prematurely terminate iterations
- **Lower-fidelity models:** Neglect physical phenomena, coarsen the mesh, or use lower-order finite differences or elements
- **Reduced-order models:** Approximate solution with a linear combination of $m_u \ll N_u$ basis functions



Solution Approximations

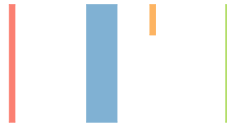
- **Inexact solutions:** When solving nonlinear equations, prematurely terminate iterations
- **Lower-fidelity models:** Neglect physical phenomena, coarsen the mesh, or use lower-order finite differences or elements
- **Reduced-order models:** Approximate solution with a linear combination of $m_u \ll N_u$ basis functions



Solution Approximations

- **Inexact solutions:** When solving nonlinear equations, prematurely terminate iterations
- **Lower-fidelity models:** Neglect physical phenomena, coarsen the mesh, or use lower-order finite differences or elements
- **Reduced-order models:** Approximate solution with a linear combination of $m_{\mathbf{u}} \ll N_{\mathbf{u}}$ basis functions

$$\tilde{\mathbf{u}}(\boldsymbol{\mu}) = \Phi_{\mathbf{u}} \hat{\mathbf{u}}(\boldsymbol{\mu}) + \bar{\mathbf{u}}$$



Parameterized Systems of Nonlinear Equations

- Parameterized systems of nonlinear equations

$$\mathbf{r}(\mathbf{u}(\boldsymbol{\mu}); \boldsymbol{\mu}) = \mathbf{0}$$

- $\mathbf{r} : \mathbb{R}^{N_{\mathbf{u}}} \times \mathbb{R}^{N_{\boldsymbol{\mu}}} \rightarrow \mathbb{R}^{N_{\mathbf{u}}}$ residual, nonlinear in at least $\mathbf{u}(\boldsymbol{\mu})$
 - $\mathbf{u} : \mathbb{R}^{N_{\boldsymbol{\mu}}} \rightarrow \mathbb{R}^{N_{\mathbf{u}}}$ state (solution vector)
 - $\boldsymbol{\mu} \in \mathcal{D}$ parameters in parameter domain $\mathcal{D} \subseteq \mathbb{R}^{N_{\boldsymbol{\mu}}}$
-
- Scalar-valued quantity of interest

$$s(\boldsymbol{\mu}) := g(\mathbf{u}(\boldsymbol{\mu}))$$

- $s : \mathbb{R}^{N_{\boldsymbol{\mu}}} \rightarrow \mathbb{R}$ quantity of interest
- $g : \mathbb{R}^{N_{\mathbf{u}}} \rightarrow \mathbb{R}$ quantity of interest functional

Error Model Construction Steps

1) Feature engineering

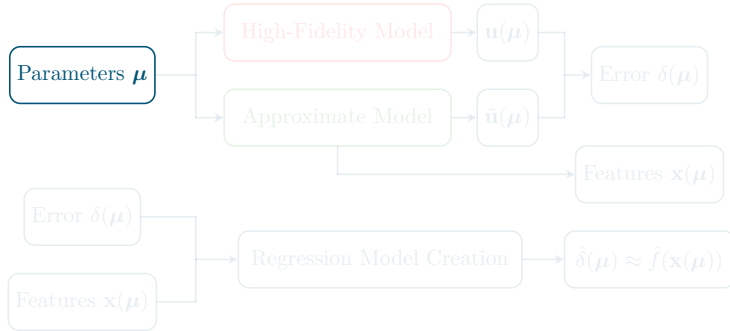
- Cheaply computable features \mathbf{x} from approximate model
- Informative of the error – construct low-noise-variance model
- Low dimensional (small $N_{\mathbf{x}}$) such that less training data are needed

2) Regression-function approximation

- Construct \hat{f} using regression methods from machine learning
- Approximate mapping from features \mathbf{x} to error δ using a training set

Summary

Training

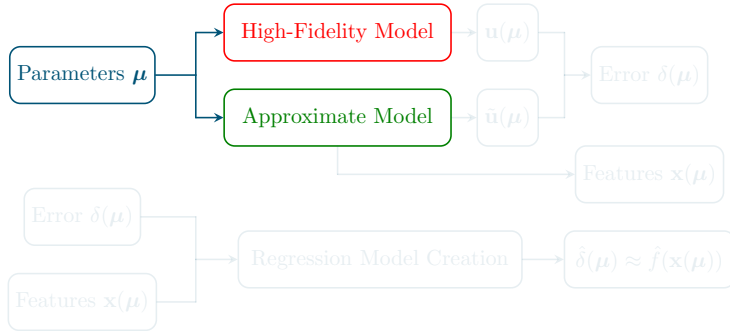


Application



Summary

Training

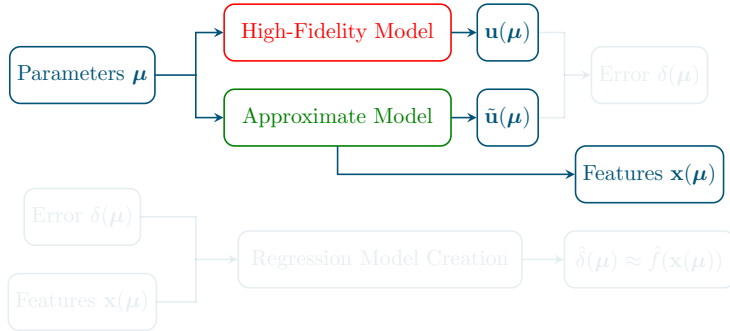


Application

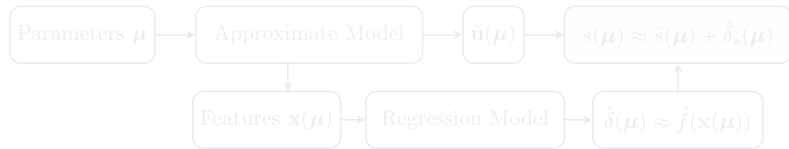


Summary

Training

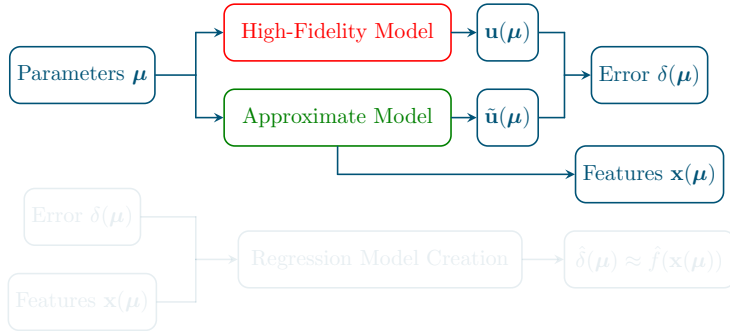


Application



Summary

Training

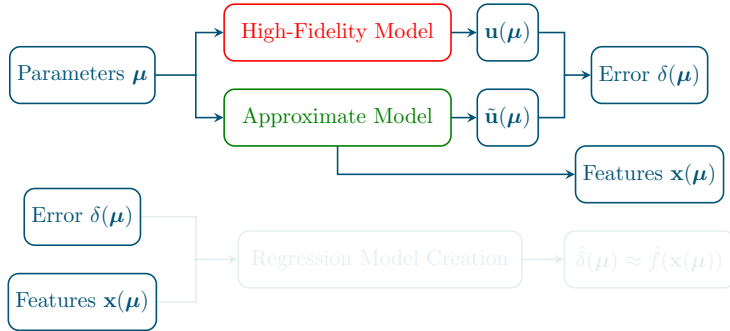


Application

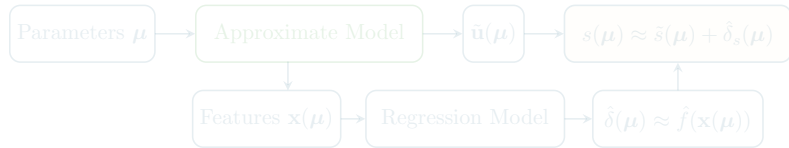


Summary

Training

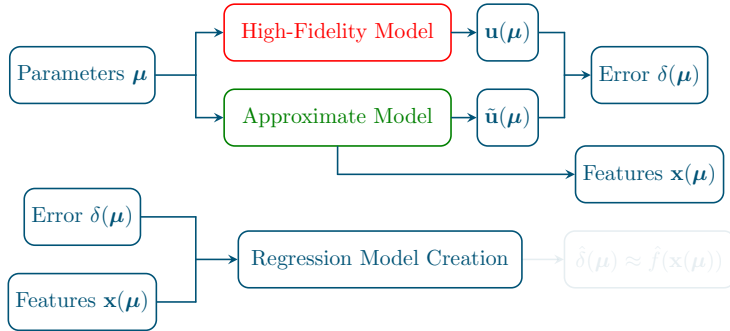


Application

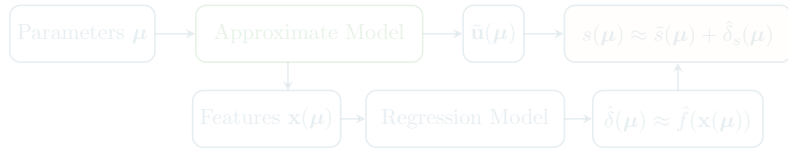


Summary

Training

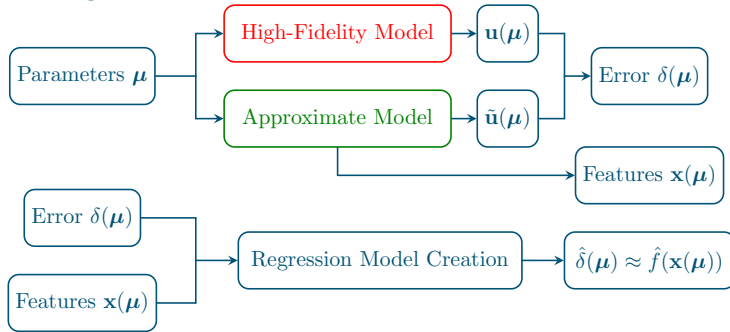


Application

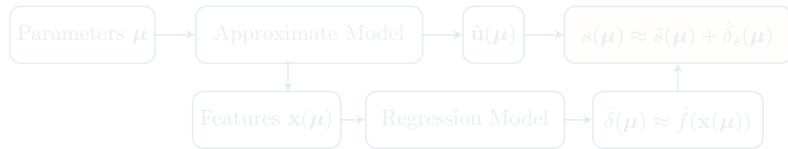


Summary

Training

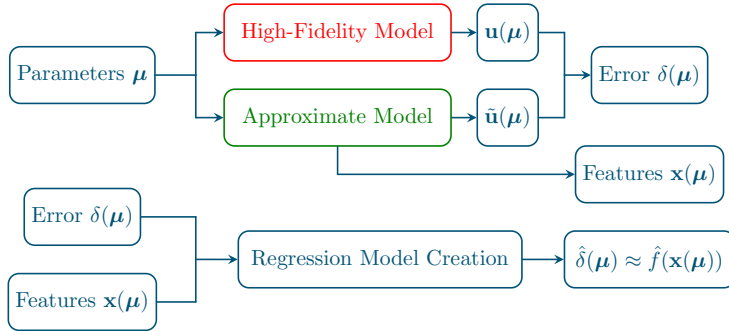


Application



Summary

Training

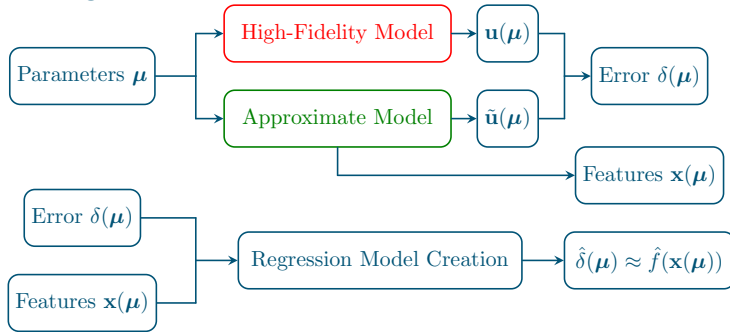


Application

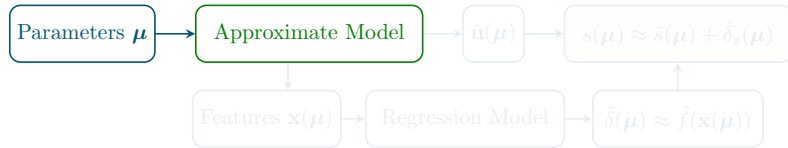


Summary

Training

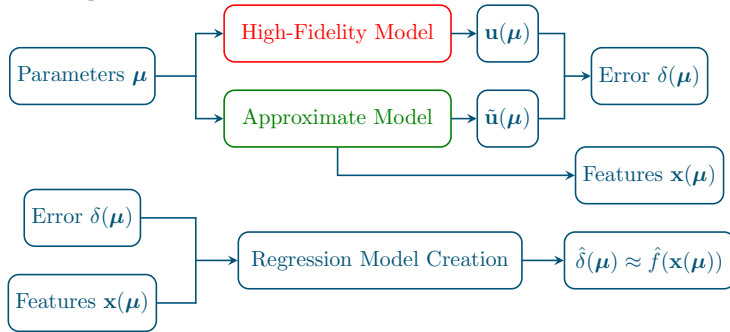


Application

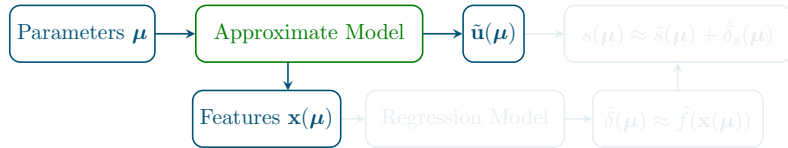


Summary

Training

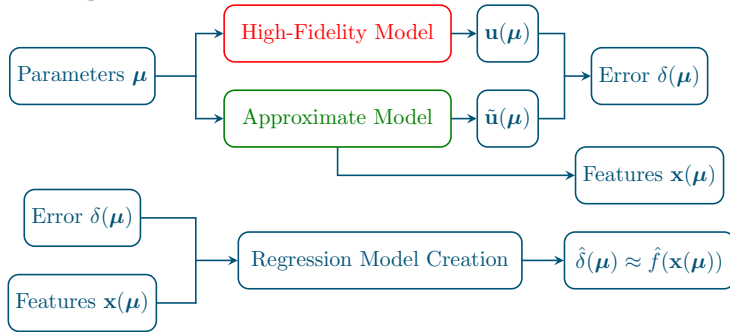


Application

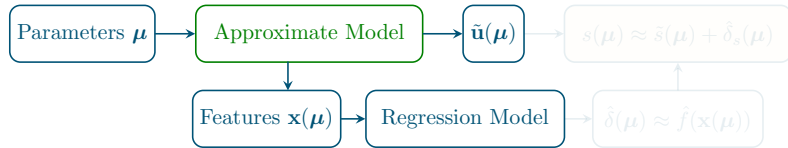


Summary

Training

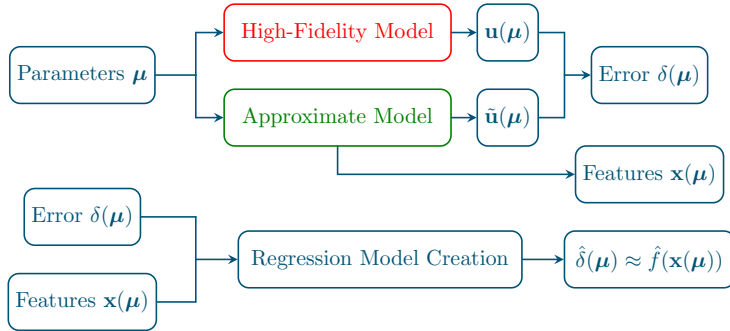


Application

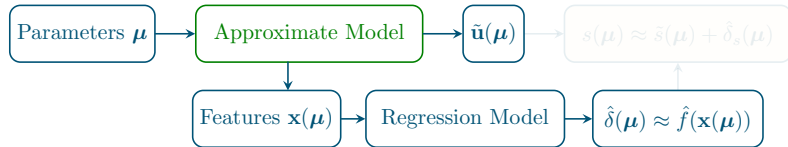


Summary

Training

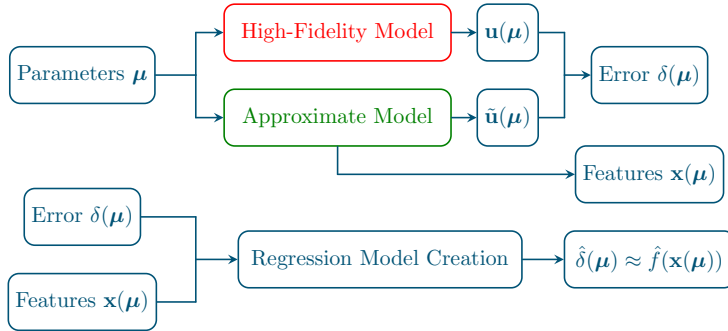


Application

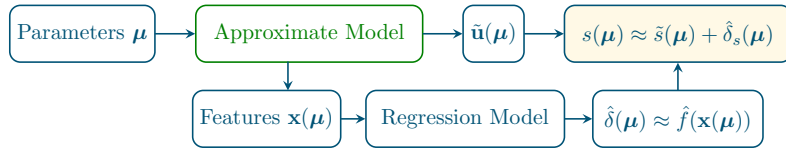


Summary

Training



Application



Dual-Weighted Residual

Approximate residual about approximate solution $\tilde{\mathbf{u}}$:

$$\mathbf{r}(\mathbf{u}(\boldsymbol{\mu}); \boldsymbol{\mu}) = \mathbf{0} = \underbrace{\mathbf{r}(\tilde{\mathbf{u}}(\boldsymbol{\mu}); \boldsymbol{\mu})}_{\mathbf{r}(\boldsymbol{\mu})} + \underbrace{\frac{\partial \mathbf{r}}{\partial \mathbf{v}}(\tilde{\mathbf{u}}(\boldsymbol{\mu}); \boldsymbol{\mu})}_{\mathbf{J}(\boldsymbol{\mu})} \underbrace{(\mathbf{u}(\boldsymbol{\mu}) - \tilde{\mathbf{u}}(\boldsymbol{\mu}))}_{\mathbf{e}(\boldsymbol{\mu})} + \mathcal{O}(\|\mathbf{e}(\boldsymbol{\mu})\|^2)$$

Rearrange to approximate state-space error: $\mathbf{e}(\boldsymbol{\mu}) = -\mathbf{J}(\boldsymbol{\mu})^{-1}\mathbf{r}(\boldsymbol{\mu}) + \mathcal{O}(\|\mathbf{e}(\boldsymbol{\mu})\|^2)$ (1)

Approximate quantity of interest about $\tilde{\mathbf{u}}$: $s(\boldsymbol{\mu}) = \tilde{s}(\boldsymbol{\mu}) + \underbrace{\frac{\partial g}{\partial \mathbf{v}}(\tilde{\mathbf{u}}(\boldsymbol{\mu}))}_{\mathbf{y}(\boldsymbol{\mu})^T}$ $\mathbf{e}(\boldsymbol{\mu}) + \mathcal{O}(\|\mathbf{e}(\boldsymbol{\mu})\|^2)$

Combine with state-space error approximation (1):

$$\delta_s(\boldsymbol{\mu}) = \underbrace{-\frac{\partial g}{\partial \mathbf{v}}(\tilde{\mathbf{u}}(\boldsymbol{\mu}))\mathbf{J}(\boldsymbol{\mu})^{-1}\mathbf{r}(\boldsymbol{\mu})}_{\mathbf{y}(\boldsymbol{\mu})^T: \text{dual or adjoint}} + \mathcal{O}(\|\mathbf{e}(\boldsymbol{\mu})\|^2)$$

Dual-weighted residual d is weighted sum of residual elements:

$$d(\boldsymbol{\mu}) := \mathbf{y}(\boldsymbol{\mu})^T \mathbf{r}(\boldsymbol{\mu}) = \sum_{i=1}^{N_u} y_i(\boldsymbol{\mu}) r_i(\boldsymbol{\mu})$$

Drawbacks to using the Dual-Weighted Residual

- **Computational Cost:** requires solving $N_{\mathbf{u}}$ linear equations
- **Implementation:** requires Jacobian – not always available

Nonetheless, structure provides insight into quantity-of-interest error

Feature Engineering: Parameters

$$\mathbf{x}(\mu) = \mu$$

- The mapping $\mu \mapsto \delta(\mu)$ is deterministic, but often complex
 - Can be oscillatory for ROMs since $\delta(\mu) \approx 0$ when $\mu \in \mathcal{D}_{\text{Train}}^{\text{ROM}}$
 - Inspired by ‘multifidelity correction’ methods for optimization

Alexandrov et al., 2001; Gano et al., 2005; Eldred et al., 2004

Feature Engineering: Dual-Weighted Residual

$$\mathbf{x}(\boldsymbol{\mu}) = d(\boldsymbol{\mu}) := \mathbf{y}(\boldsymbol{\mu})^T \mathbf{r}(\boldsymbol{\mu})$$

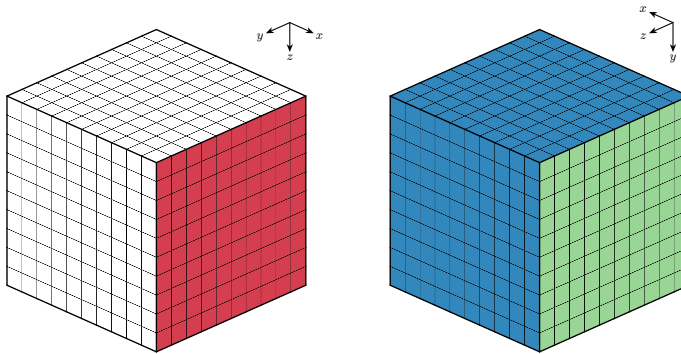
- First-order approximation of QoI error $\delta_s(\boldsymbol{\mu})$
- Small number ($N_{\mathbf{x}} = 1$) of high-quality features
- High computational cost and significant implementation effort

Feature Engineering: Parameters and Residual (Approximations)

$$\mathbf{x}(\mu) = [\mu; \mathbf{r}(\mu)]$$

- DWR is weighted sum of residual vector elements $d(\boldsymbol{\mu}) := \mathbf{y}(\boldsymbol{\mu})^T \mathbf{r}(\boldsymbol{\mu})$
 - Avoids implementation and costs associated with dual vector $\mathbf{y}(\boldsymbol{\mu})$
 - Large number ($N_{\mathbf{x}} = N_{\boldsymbol{\mu}} + N_{\mathbf{u}}$) of low-quality features
 - Approaches to reduce number of features and improve quality
 - Use $m_{\mathbf{r}} \ll N_{\mathbf{u}}$ principal component coefficients: $\hat{\mathbf{r}}(\boldsymbol{\mu})$
 - Sample $n_{\mathbf{r}} \ll N_{\mathbf{u}}$ elements of residual: $\mathbf{Pr}(\boldsymbol{\mu})$, where $\mathbf{P} \in \{0, 1\}^{n_{\mathbf{r}} \times N_{\mathbf{u}}}$
 - Use $m_{\mathbf{r}} \ll N_{\mathbf{u}}$ gappy principal component coefficients: $\hat{\mathbf{r}}_g(\boldsymbol{\mu})$

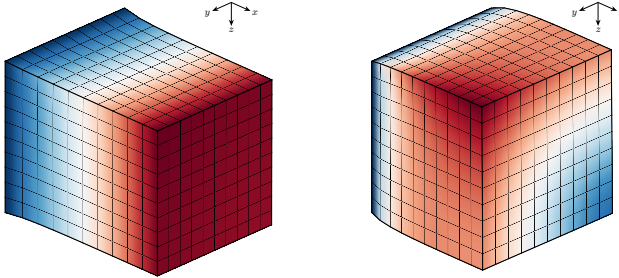
Cube: Reduced-Order Modeling



- Applied traction (Neumann boundary condition)
- Planar constraint (Dirichlet boundary condition)
- Complete constraint (Dirichlet boundary condition)
- Node of interest

Cube: Overview

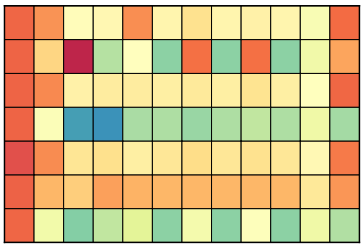
- $N_u = 3410$ – deliberately small to compute $d(\mu)$ and use $\mathbf{r}(\mu)$
- $N_\mu = 3$ parameters: $\mu = [E; \nu; t]$
 - $E \in [75, 125]$ GPa, $\nu \in [0.20, 0.35]$, $t \in [40, 60]$ GPa
- 8 HF runs \rightarrow up to $m_u = 8$ ROM basis vectors (2 used – 99.49%)



Cube: Variance Unexplained for QoI Error Prediction

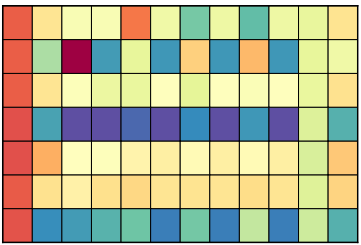
Regression Methods

$$\delta_{ux} : \log_{10} (1 - r^2)$$



Features

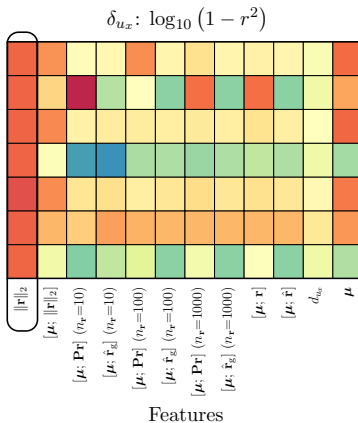
$$\delta_{uy} : \log_{10} (1 - r^2)$$



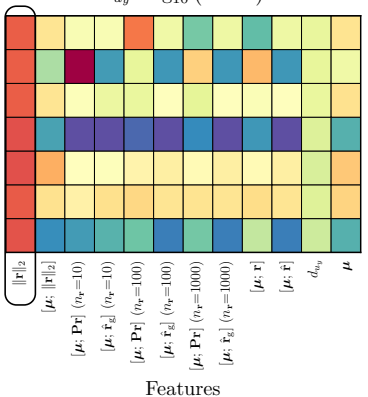
Features

Cube: Variance Unexplained for QoI Error Prediction

Regression Methods



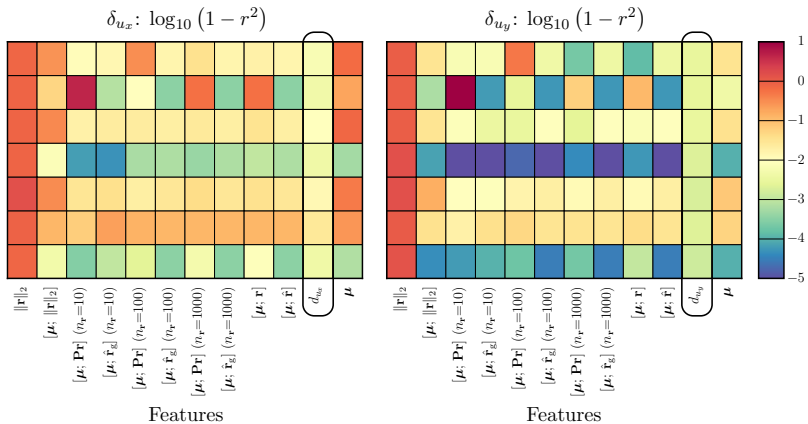
$$\delta_{uy} : \log_{10} (1 - r^2)$$



- $\|\mathbf{r}\|_2$ yields highest variance unexplained

Cube: Variance Unexplained for QoI Error Prediction

Regression Methods



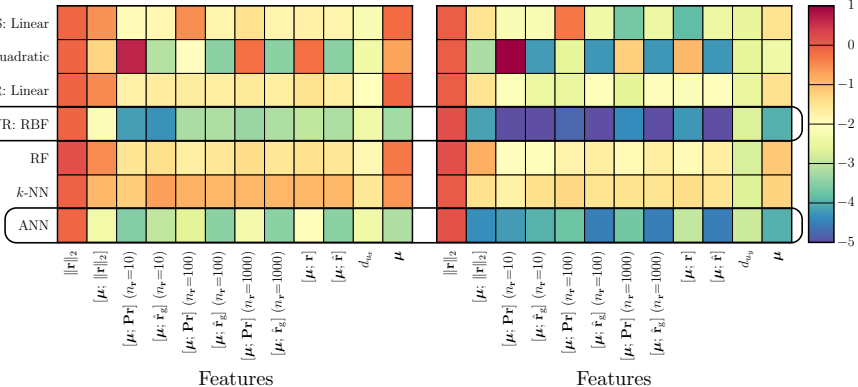
- $\|\mathbf{r}\|_2$ yields highest variance unexplained
- d_{ux} and d_{uy} yield moderate variance unexplained, but are costly

Cube: Variance Unexplained for QoI Error Prediction

Regression Methods

$$\delta_{ux} : \log_{10}(1 - r^2)$$

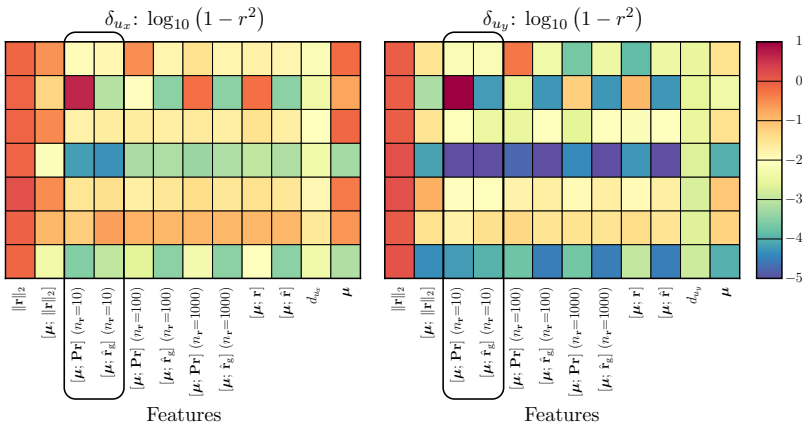
$$\delta_{uy} : \log_{10}(1 - r^2)$$



- $\|r\|_2$ yields highest variance unexplained
- d_{ux} and d_{uy} yield moderate variance unexplained, but are costly
- SVR: RBF and ANN yield lowest variance unexplained

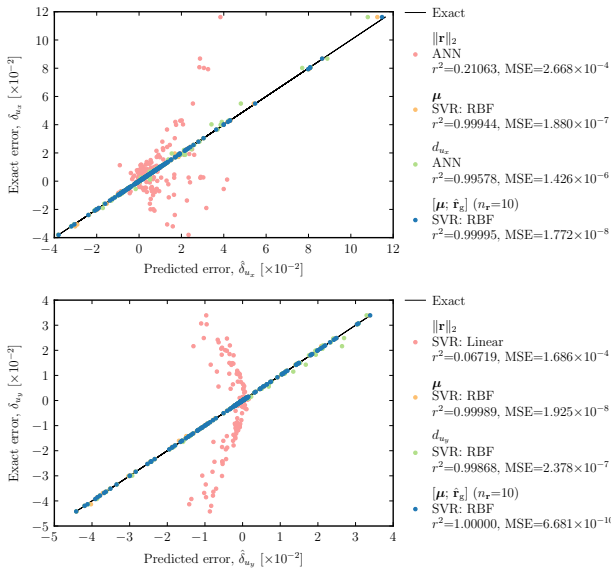
Cube: Variance Unexplained for QoI Error Prediction

Regression Methods



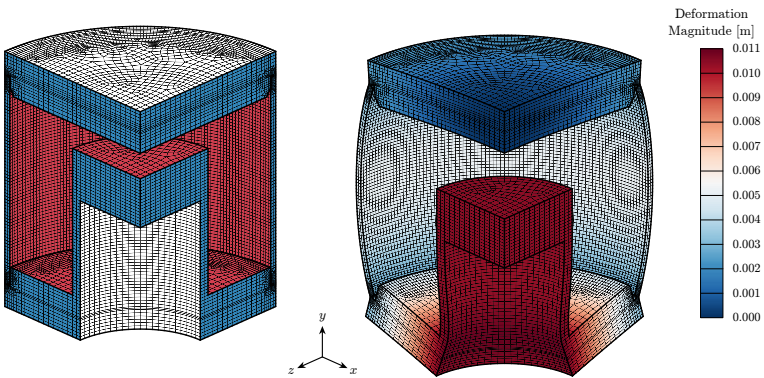
- $\|\mathbf{r}\|_2$ yields highest variance unexplained
- d_{ux} and d_{uy} yield moderate variance unexplained, but are costly
- SVR: RBF and ANN yield lowest variance unexplained
- $[\boldsymbol{\mu}; \hat{\mathbf{r}}_g]$ and $[\boldsymbol{\mu}; \mathbf{Pr}]$ yield low variance unexplained with only 10 samples (compared to $N_u = 3410$)

Cube: QoI Error Predictions



- Our method beats previous state-of-the-art methods with $r^2 > 0.9999$ in both cases

Predictive Capability Assessment Project: Reduced-Order Modeling

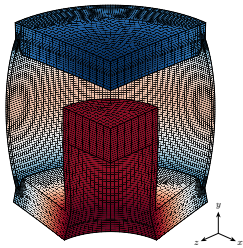


- Applied pressure (Neumann boundary condition)
- Planar constraint (Dirichlet boundary condition)
- Complete constraint (Dirichlet boundary condition)
- Nodes of interest

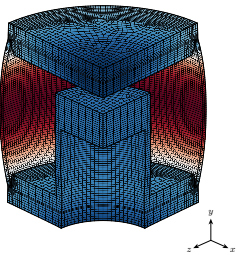
PCAP: Overview

- $N_{\mathbf{u}} = 274,954$ for quarter of domain
- $N_{\boldsymbol{\mu}} = 3$ parameters: $\boldsymbol{\mu} = [E; \nu; p]$
 - $E \in [50, 100]$ GPa, $\nu \in [0.20, 0.35]$, $p \in [6, 10]$ GPa
- 30 parameter training instances for regression model

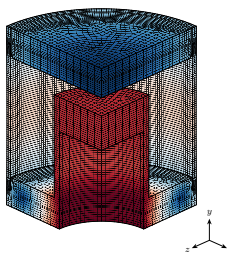
PCAP: Basis Vectors



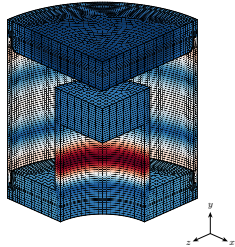
1: 85.03%



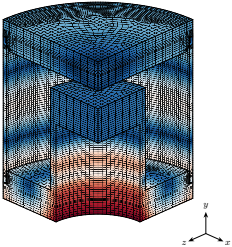
2: 95.69%



3: 99.35%



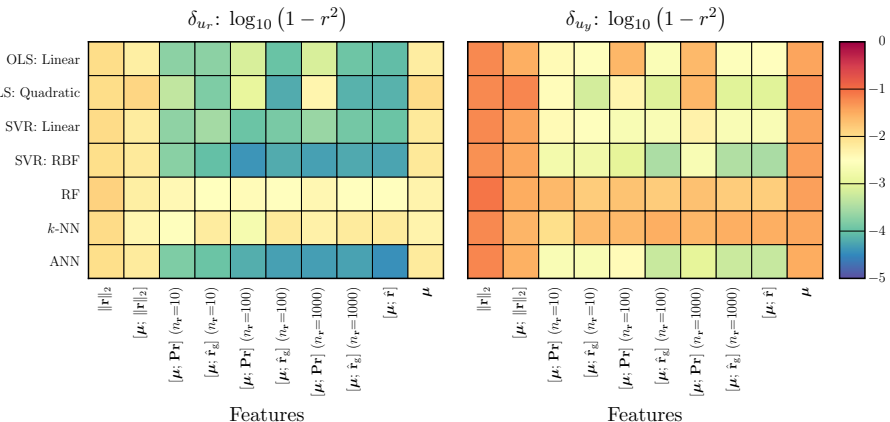
4: 99.77%



5: 99.90%

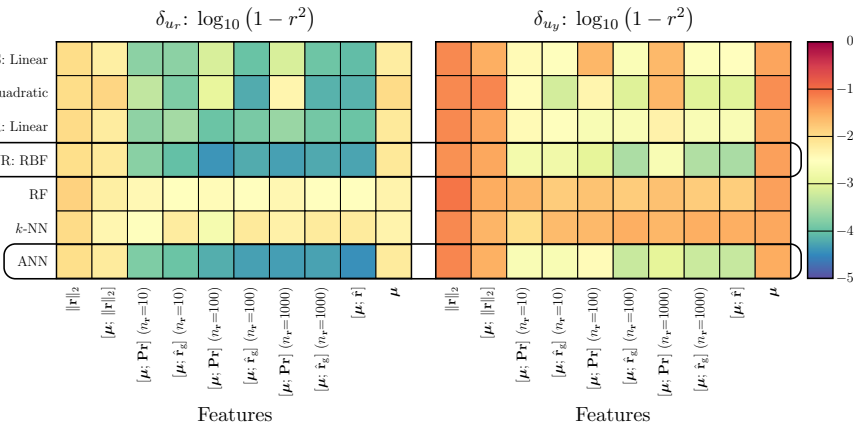
PCAP: Variance Unexplained for QoI Error Prediction

Regression Methods



PCAP: Variance Unexplained for QoI Error Prediction

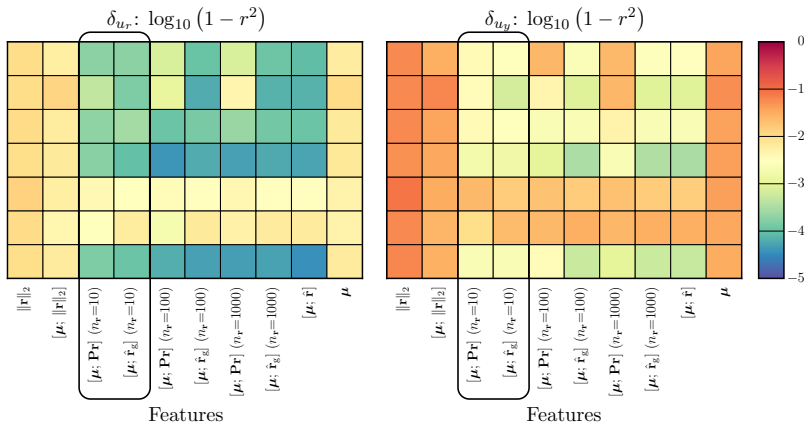
Regression Methods



- SVR: RBF and ANN yield lowest variance unexplained

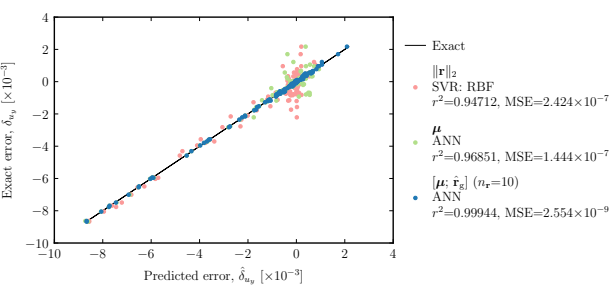
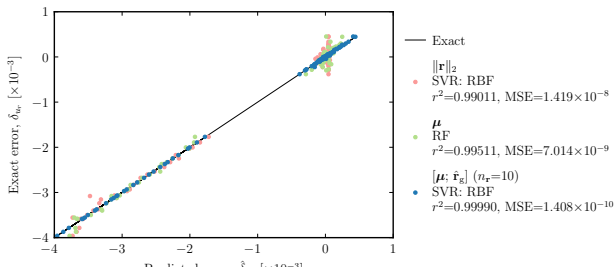
PCAP: Variance Unexplained for QoI Error Prediction

Regression Methods



- SVR: RBF and ANN yield lowest variance unexplained
- $[\boldsymbol{\mu}; \hat{\mathbf{r}}_g]$ and $[\boldsymbol{\mu}; \mathbf{Pr}]$ yield low variance unexplained with only 10 samples (compared to $N_u = 274,954$)

PCAP: QoI Error Predictions



- Our method beats previous state-of-the-art methods with $r^2 > 0.9994$ in both cases

Summary

- Accurately computed error from approximate solutions
- $r^2 > 0.996$ for all experiments
- Only used about 13 features

CODE-VERIFICATION TECHNIQUES FOR HYPERSONIC REACTING FLOWS IN THERMOCHEMICAL NONEQUILIBRIUM

Brian A. Freno

Brian R. Carnes

V. Gregory Weirs

Sandia National Laboratories

Hypersonic Flow

Hypersonic flows and underlying aerothermochemical phenomena

- Important in design & analysis of vehicles exiting/reentering atmosphere
 - High flow velocities and stagnation enthalpies
 - Induce chemical reactions
 - Excite thermal energy modes
 - Aerodynamic and thermochemical models require full coupling

Sandia Parallel Aerodynamics and Reentry Code (SPARC)

Sandia Parallel Aerodynamics and Reentry Code (SPARC)

- Compressible computational fluids dynamics code
 - Actively under development at Sandia National Laboratories
 - Models transonic and hypersonic reacting turbulent flows
 - Solves transient heat equation and equations associated with decomposing and non-decomposing ablation
 - One- and two-way couplings between fluid dynamics and ablation

Verification and Validation

Credibility of computational physics codes requires verification and validation

- **Validation** assesses how well models represent physical phenomena
 - Compare computational results with experimental results
 - Assess suitability of models, model error, and bounds of validity
- **Verification** assesses accuracy of numerical solutions against expectations
 - *Solution verification* estimates numerical error for particular solution
 - *Code verification* assesses correctness of numerical-method implementation

Code verification is the focus of this part

Code Verification

Code verification assesses correctness of numerical-method implementation

- Continuous equations are numerically **discretized**

$$\mathbf{r}(\mathbf{u}) = \mathbf{0} \quad \rightarrow \quad \mathbf{r}_h(\mathbf{u}_h) = \mathbf{0}$$

- Discretization error is introduced in solution

$$\mathbf{e} = \mathbf{u}_h - \mathbf{u}$$

- Discretization error should decrease as discretization is refined

$$\lim_{h \rightarrow 0} \mathbf{e} = \mathbf{0}$$

- More rigorously, should decrease at an expected rate

$$\|\mathbf{e}\| \approx Ch^p$$

- Measuring error requires exact solution – usually unavailable

Manufactured Solutions: Overview

Manufactured solutions are popular alternative

- Manufacture an arbitrary solution \mathbf{u}_{MS}
 - Insert manufactured solution into continuous equations to get residual term

$$\mathbf{r}(\mathbf{u}_{\text{MS}}) \neq \mathbf{0}$$

- Add residual term to discretized equations

$$\mathbf{r}_h(\mathbf{u}_h) = \mathbf{r}(\mathbf{u}_{\text{MS}})$$

to coerce solution to manufactured solution

$$\mathbf{u}_h \rightarrow \mathbf{u}_{\text{MS}}$$

Manufactured Solutions: An Example

Consider Laplace's equation in 1D $r(u) = \frac{\partial^2 u}{\partial x^2} = 0$

Discretized by finite differences

$$r_h(u_h) = \frac{u_{i+1} - 2u_i + u_{i-1}}{\Delta x^2} = 0$$

Manufacture the arbitrary solution $u_{\text{MS}}(x) = \sin(\pi x)$, such that

$$r(u_{\text{MS}}) = \frac{\partial^2 u_{\text{MS}}}{\partial x^2} = -\pi^2 \sin(\pi x)$$

Solve $r_h(u_h) = r(u_{\text{MS}})$, such that

$$\frac{u_{i+1} - 2u_i + u_{i-1}}{\Delta x^2} = -\pi^2 \sin(\pi x_i)$$

The discretization error is $e = u_h - u_{\text{MS}}$

Importance of Code Verification

Consequences of incorrectly implemented numerical methods:

- Wasted computational expense:
 - Numerical errors **decrease slower** with mesh refinement than they should
 - Numerical errors **do not decrease** with mesh refinement
 - Numerical solutions **differ moderately** from exact solutions
 - Numerical solutions **differ significantly** from exact solutions
 - **Application failure** from incorrect numerical results
 - Consequences may not be obvious

Benefits of code verification:

- Assess suitability and correctness of numerical methods
 - Compare accuracy of different algorithms
 - Set expectations and estimate error for solution verification

Code Verification Scope

Code verification demonstrated in many computational physics disciplines

- Fluid dynamics
- Multiphase flows
- Fluid–structure interaction
- Solid mechanics
- Electrodynamics
- Radiation hydrodynamics
- Heat transfer
- Electromagnetism

Code-verification techniques for hypersonic flows have been presented

- Single-species perfect gas
- Multi-species gas in thermal equilibrium

We present code-verification techniques for hypersonic reacting flows in thermochemical **nonequilibrium** and demonstrate effectiveness

- Spatial discretization
- Thermochemical source term

Governing Equations: n_s Species in Vibrational Nonequilibrium

Conservation of mass, momentum, and energy:

$$\frac{\partial \mathbf{u}}{\partial t} + \nabla \cdot \mathbf{F}_c(\mathbf{u}) = -\nabla \cdot \mathbf{F}_p(\mathbf{u}) + \nabla \cdot \mathbf{F}_d(\mathbf{u}) + \mathbf{S}(\mathbf{u}),$$

where

$$\mathbf{u} = \begin{Bmatrix} \rho \\ \rho\mathbf{v} \\ \rho E \\ \rho e_v \end{Bmatrix}, \quad \mathbf{F}_c(\mathbf{u}) = \begin{Bmatrix} \rho\mathbf{v}^T \\ \rho\mathbf{v}\mathbf{v}^T \\ \rho E\mathbf{v}^T \\ \rho e_v\mathbf{v}^T \end{Bmatrix}, \quad \mathbf{F}_p(\mathbf{u}) = \begin{Bmatrix} \mathbf{0} \\ p\mathbf{I} \\ p\mathbf{v}^T \\ \mathbf{0}^T \end{Bmatrix}, \quad \mathbf{F}_d(\mathbf{u}) = \begin{Bmatrix} -\mathbf{J} \\ \boldsymbol{\tau} \\ (\boldsymbol{\tau}\mathbf{v} - \mathbf{q} - \mathbf{q}_v - \mathbf{J}^T\mathbf{h})^T \\ (-\mathbf{q}_v - \mathbf{J}^T\mathbf{e}_v)^T \end{Bmatrix},$$

$$\mathbf{S}(\mathbf{u}) = \begin{Bmatrix} \dot{\mathbf{w}} \\ \mathbf{0} \\ 0 \\ Q_{t-v} + \mathbf{e}_v^T \dot{\mathbf{w}} \end{Bmatrix}, \quad \begin{aligned} \boldsymbol{\rho} &= \{\rho_1, \dots, \rho_{n_s}\}^T, & \dot{\mathbf{w}} &= \{\dot{w}_1, \dots, \dot{w}_{n_s}\}^T: \text{mass production rates per volume,} \\ \rho &= \sum_{s=1}^{n_s} \rho_s, & e_v &= \sum_{s=1}^{n_s} \frac{\rho_s}{\rho} e_{v_s}: \text{mixture vibrational energy per mass,} \\ p &= \sum_{s=1}^{n_s} \frac{\rho_s}{M_s} \bar{R}T, & \mathbf{e}_v &= \{e_{v_1}, \dots, e_{v_{n_s}}\}^T: \text{vibrational energies per mass,} \\ Q_{t-v} &: \text{translational-vibrational energy exchange,} \end{aligned}$$

$$E = \frac{|\mathbf{v}|^2}{2} + \sum_{s=1}^{n_s} \frac{\rho_s}{\rho} (c_{v_s} T + e_{v_s} + h_s^o)$$

Governing Equations: n_s Species in Vibrational Nonequilibrium

Conservation of mass, momentum, and energy:

$$\frac{\partial \mathbf{u}}{\partial t} + \nabla \cdot \mathbf{F}_c(\mathbf{u}) = -\nabla \cdot \mathbf{F}_p(\mathbf{u}) + \nabla \cdot \mathbf{F}_d(\mathbf{u}) + \mathbf{S}(\mathbf{u}),$$

where

$$\mathbf{u} = \begin{Bmatrix} \rho \\ \rho \mathbf{v} \\ \rho E \\ \rho e_v \end{Bmatrix}, \quad \mathbf{F}_c(\mathbf{u}) = \begin{Bmatrix} \rho \mathbf{v}^T \\ \rho \mathbf{v} \mathbf{v}^T \\ \rho E \mathbf{v}^T \\ \rho e_v \mathbf{v}^T \end{Bmatrix}, \quad \mathbf{F}_p(\mathbf{u}) = \begin{Bmatrix} \mathbf{0} \\ p \mathbf{I} \\ p \mathbf{v}^T \\ \mathbf{0}^T \end{Bmatrix}, \quad \mathbf{F}_d(\mathbf{u}) = \begin{Bmatrix} -\mathbf{J} \\ \boldsymbol{\tau} \\ (\tau \mathbf{v} - \mathbf{q} - \mathbf{q}_v - \mathbf{J}^T \mathbf{h})^T \\ (-\mathbf{q}_v - \mathbf{J}^T \mathbf{e}_v)^T \end{Bmatrix},$$

Multiple species

$$\mathbf{S}(\mathbf{u}) = \begin{Bmatrix} \dot{\mathbf{w}} \\ \mathbf{0} \\ \mathbf{0} \\ Q_{t-v} + \mathbf{e}_v^T \dot{\mathbf{w}} \end{Bmatrix}, \quad \begin{aligned} \mathbf{p} &= \{\rho_1, \dots, \rho_{n_s}\}^T, & \dot{\mathbf{w}} &= \{\dot{w}_1, \dots, \dot{w}_{n_s}\}^T: \text{mass production rates per volume,} \\ \rho &= \sum_{s=1}^{n_s} \rho_s, & e_v &= \sum_{s=1}^{n_s} \frac{\rho_s}{\rho} e_{v_s}: \text{mixture vibrational energy per mass,} \\ p &= \sum_{s=1}^{n_s} \frac{\rho_s}{M_s} \bar{R} T, & \mathbf{e}_v &= \{e_{v_1}, \dots, e_{v_{n_s}}\}^T: \text{vibrational energies per mass,} \\ Q_{t-v} &: \text{translational-vibrational energy exchange,} \end{aligned}$$

$$E = \frac{|\mathbf{v}|^2}{2} + \sum_{s=1}^{n_s} \frac{\rho_s}{\rho} (c_{v_s} T + e_{v_s} + h_s^o)$$

Governing Equations: n_s Species in Vibrational Nonequilibrium

Conservation of mass, momentum, and energy:

Local time derivative

$$\frac{\partial \mathbf{u}}{\partial t} + \nabla \cdot \mathbf{F}_c(\mathbf{u}) = -\nabla \cdot \mathbf{F}_p(\mathbf{u}) + \nabla \cdot \mathbf{F}_d(\mathbf{u}) + \mathbf{S}(\mathbf{u}),$$

where

$$\mathbf{u} = \begin{Bmatrix} \rho \\ \rho \mathbf{v} \\ \rho E \\ \rho e_v \end{Bmatrix}, \quad \mathbf{F}_c(\mathbf{u}) = \begin{Bmatrix} \rho \mathbf{v}^T \\ \rho \mathbf{v} \mathbf{v}^T \\ \rho E \mathbf{v}^T \\ \rho e_v \mathbf{v}^T \end{Bmatrix}, \quad \mathbf{F}_p(\mathbf{u}) = \begin{Bmatrix} \mathbf{0} \\ p \mathbf{I} \\ p \mathbf{v}^T \\ \mathbf{0}^T \end{Bmatrix}, \quad \mathbf{F}_d(\mathbf{u}) = \begin{Bmatrix} -\mathbf{J} \\ \tau \\ (\tau \mathbf{v} - \mathbf{q} - \mathbf{q}_v - \mathbf{J}^T \mathbf{h})^T \\ (-\mathbf{q}_v - \mathbf{J}^T \mathbf{e}_v)^T \end{Bmatrix},$$

$$\mathbf{S}(\mathbf{u}) = \begin{Bmatrix} \dot{\mathbf{w}} \\ \mathbf{0} \\ \mathbf{0} \\ Q_{t-v} + \mathbf{e}_v^T \dot{\mathbf{w}} \end{Bmatrix}, \quad \begin{aligned} \rho &= \{\rho_1, \dots, \rho_{n_s}\}^T, & \dot{\mathbf{w}} &= \{\dot{w}_1, \dots, \dot{w}_{n_s}\}^T: \text{mass production rates per volume,} \\ \rho &= \sum_{s=1}^{n_s} \rho_s, & e_v &= \sum_{s=1}^{n_s} \frac{\rho_s}{\rho} e_{v_s}: \text{mixture vibrational energy per mass,} \\ p &= \sum_{s=1}^{n_s} \frac{\rho_s}{M_s} \bar{R} T, & \mathbf{e}_v &= \{e_{v_1}, \dots, e_{v_{n_s}}\}^T: \text{vibrational energies per mass,} \\ Q_{t-v} &: \text{translational-vibrational energy exchange,} \end{aligned}$$

$$E = \frac{|\mathbf{v}|^2}{2} + \sum_{s=1}^{n_s} \frac{\rho_s}{\rho} (c_{v_s} T + e_{v_s} + h_s^o)$$

Governing Equations: n_s Species in Vibrational Nonequilibrium

Conservation of mass, momentum, and energy:

Convective flux gradient

$$\frac{\partial \mathbf{u}}{\partial t} + \nabla \cdot \mathbf{F}_c(\mathbf{u}) = -\nabla \cdot \mathbf{F}_p(\mathbf{u}) + \nabla \cdot \mathbf{F}_d(\mathbf{u}) + \mathbf{S}(\mathbf{u}),$$

where

$$\mathbf{u} = \begin{Bmatrix} \rho \\ \rho \mathbf{v} \\ \rho E \\ \rho e_v \end{Bmatrix}, \quad \mathbf{F}_c(\mathbf{u}) = \begin{Bmatrix} \rho \mathbf{v}^T \\ \rho \mathbf{v} \mathbf{v}^T \\ \rho E \mathbf{v}^T \\ \rho e_v \mathbf{v}^T \end{Bmatrix}, \quad \mathbf{F}_p(\mathbf{u}) = \begin{Bmatrix} \mathbf{0} \\ p \mathbf{I} \\ p \mathbf{v}^T \\ \mathbf{0}^T \end{Bmatrix}, \quad \mathbf{F}_d(\mathbf{u}) = \begin{Bmatrix} -\mathbf{J} \\ \tau \\ (\tau \mathbf{v} - \mathbf{q} - \mathbf{q}_v - \mathbf{J}^T \mathbf{h})^T \\ (-\mathbf{q}_v - \mathbf{J}^T \mathbf{e}_v)^T \end{Bmatrix},$$

$$\mathbf{S}(\mathbf{u}) = \begin{Bmatrix} \dot{\mathbf{w}} \\ \mathbf{0} \\ \mathbf{0} \\ Q_{t-v} + \mathbf{e}_v^T \dot{\mathbf{w}} \end{Bmatrix}, \quad \begin{aligned} \rho &= \{\rho_1, \dots, \rho_{n_s}\}^T, & \dot{\mathbf{w}} &= \{\dot{w}_1, \dots, \dot{w}_{n_s}\}^T: \text{mass production rates per volume,} \\ \rho &= \sum_{s=1}^{n_s} \rho_s, & e_v &= \sum_{s=1}^{n_s} \frac{\rho_s}{\rho} e_{v_s}: \text{mixture vibrational energy per mass,} \\ p &= \sum_{s=1}^{n_s} \frac{\rho_s}{M_s} \bar{R} T, & \mathbf{e}_v &= \{e_{v_1}, \dots, e_{v_{n_s}}\}^T: \text{vibrational energies per mass,} \\ Q_{t-v} &: \text{translational-vibrational energy exchange,} \end{aligned}$$

$$E = \frac{|\mathbf{v}|^2}{2} + \sum_{s=1}^{n_s} \frac{\rho_s}{\rho} (c_{v_s} T + e_{v_s} + h_s^o)$$

Governing Equations: n_s Species in Vibrational Nonequilibrium

Conservation of mass, momentum, and energy:

Pressure flux gradient

$$\frac{\partial \mathbf{u}}{\partial t} + \nabla \cdot \mathbf{F}_c(\mathbf{u}) = -\nabla \cdot \mathbf{F}_p(\mathbf{u}) + \nabla \cdot \mathbf{F}_d(\mathbf{u}) + \mathbf{S}(\mathbf{u}),$$

where

$$\mathbf{u} = \begin{Bmatrix} \rho \\ \rho \mathbf{v} \\ \rho E \\ \rho e_v \end{Bmatrix}, \quad \mathbf{F}_c(\mathbf{u}) = \begin{Bmatrix} \rho \mathbf{v}^T \\ \rho \mathbf{v} \mathbf{v}^T \\ \rho E \mathbf{v}^T \\ \rho e_v \mathbf{v}^T \end{Bmatrix}, \quad \mathbf{F}_p(\mathbf{u}) = \begin{Bmatrix} \mathbf{0} \\ p \mathbf{I} \\ p \mathbf{v}^T \\ \mathbf{0}^T \end{Bmatrix}, \quad \mathbf{F}_d(\mathbf{u}) = \begin{Bmatrix} -\mathbf{J} \\ \tau \\ (\tau \mathbf{v} - \mathbf{q} - \mathbf{q}_v - \mathbf{J}^T \mathbf{h})^T \\ (-\mathbf{q}_v - \mathbf{J}^T \mathbf{e}_v)^T \end{Bmatrix},$$

$$\mathbf{S}(\mathbf{u}) = \begin{Bmatrix} \dot{\mathbf{w}} \\ \mathbf{0} \\ 0 \\ Q_{t-v} + \mathbf{e}_v^T \dot{\mathbf{w}} \end{Bmatrix}, \quad \begin{aligned} \rho &= \{\rho_1, \dots, \rho_{n_s}\}^T, & \dot{\mathbf{w}} &= \{\dot{w}_1, \dots, \dot{w}_{n_s}\}^T: \text{mass production rates per volume,} \\ \rho &= \sum_{s=1}^{n_s} \rho_s, & e_v &= \sum_{s=1}^{n_s} \frac{\rho_s}{\rho} e_{v_s}: \text{mixture vibrational energy per mass,} \\ p &= \sum_{s=1}^{n_s} \frac{\rho_s}{M_s} \bar{R} T, & \mathbf{e}_v &= \{e_{v_1}, \dots, e_{v_{n_s}}\}^T: \text{vibrational energies per mass,} \\ Q_{t-v} &: \text{translational-vibrational energy exchange,} \end{aligned}$$

$$E = \frac{|\mathbf{v}|^2}{2} + \sum_{s=1}^{n_s} \frac{\rho_s}{\rho} (c_{V_s} T + e_{v_s} + h_s^o)$$

Governing Equations: n_s Species in Vibrational Nonequilibrium

Conservation of mass, momentum, and energy:

Diffusive flux gradient

$$\frac{\partial \mathbf{u}}{\partial t} + \nabla \cdot \mathbf{F}_c(\mathbf{u}) = -\nabla \cdot \mathbf{F}_p(\mathbf{u}) + \nabla \cdot \mathbf{F}_d(\mathbf{u}) + \mathbf{S}(\mathbf{u}),$$

where

$$\mathbf{u} = \begin{Bmatrix} \rho \\ \rho \mathbf{v} \\ \rho E \\ \rho e_v \end{Bmatrix}, \quad \mathbf{F}_c(\mathbf{u}) = \begin{Bmatrix} \rho \mathbf{v}^T \\ \rho \mathbf{v} \mathbf{v}^T \\ \rho E \mathbf{v}^T \\ \rho e_v \mathbf{v}^T \end{Bmatrix}, \quad \mathbf{F}_p(\mathbf{u}) = \begin{Bmatrix} \mathbf{0} \\ p \mathbf{I} \\ p \mathbf{v}^T \\ \mathbf{0}^T \end{Bmatrix}, \quad \mathbf{F}_d(\mathbf{u}) = \begin{Bmatrix} -\mathbf{J} \\ \boldsymbol{\tau} \\ (\boldsymbol{\tau} \mathbf{v} - \mathbf{q} - \mathbf{q}_v - \mathbf{J}^T \mathbf{h})^T \\ (-\mathbf{q}_v - \mathbf{J}^T \mathbf{e}_v)^T \end{Bmatrix},$$

$$\mathbf{S}(\mathbf{u}) = \begin{Bmatrix} \dot{\mathbf{w}} \\ \mathbf{0} \\ \mathbf{0} \\ Q_{t-v} + \mathbf{e}_v^T \dot{\mathbf{w}} \end{Bmatrix}, \quad \begin{aligned} \rho &= \{\rho_1, \dots, \rho_{n_s}\}^T, & \dot{\mathbf{w}} &= \{\dot{w}_1, \dots, \dot{w}_{n_s}\}^T: \text{mass production rates per volume,} \\ \rho &= \sum_{s=1}^{n_s} \rho_s, & e_v &= \sum_{s=1}^{n_s} \frac{\rho_s}{\rho} e_{v_s}: \text{mixture vibrational energy per mass,} \\ p &= \sum_{s=1}^{n_s} \frac{\rho_s}{M_s} \bar{R} T, & \mathbf{e}_v &= \{e_{v_1}, \dots, e_{v_{n_s}}\}^T: \text{vibrational energies per mass,} \\ Q_{t-v} &: \text{translational-vibrational energy exchange,} \end{aligned}$$

$$E = \frac{|\mathbf{v}|^2}{2} + \sum_{s=1}^{n_s} \frac{\rho_s}{\rho} (c_{v_s} T + e_{v_s} + h_s^o)$$

Governing Equations: n_s Species in Vibrational Nonequilibrium

Conservation of mass, momentum, and energy:

Thermochemical source term

$$\frac{\partial \mathbf{u}}{\partial t} + \nabla \cdot \mathbf{F}_c(\mathbf{u}) = -\nabla \cdot \mathbf{F}_p(\mathbf{u}) + \nabla \cdot \mathbf{F}_d(\mathbf{u}) + \mathbf{S}(\mathbf{u}),$$

where

$$\mathbf{u} = \begin{Bmatrix} \rho \\ \rho \mathbf{v} \\ \rho E \\ \rho e_v \end{Bmatrix}, \quad \mathbf{F}_c(\mathbf{u}) = \begin{Bmatrix} \rho \mathbf{v}^T \\ \rho \mathbf{v} \mathbf{v}^T \\ \rho E \mathbf{v}^T \\ \rho e_v \mathbf{v}^T \end{Bmatrix}, \quad \mathbf{F}_p(\mathbf{u}) = \begin{Bmatrix} \mathbf{0} \\ p \mathbf{I} \\ p \mathbf{v}^T \\ \mathbf{0}^T \end{Bmatrix}, \quad \mathbf{F}_d(\mathbf{u}) = \begin{Bmatrix} -\mathbf{J} \\ \tau \\ (\tau \mathbf{v} - \mathbf{q} - \mathbf{q}_v - \mathbf{J}^T \mathbf{h})^T \\ (-\mathbf{q}_v - \mathbf{J}^T \mathbf{e}_v)^T \end{Bmatrix},$$

$$\mathbf{S}(\mathbf{u}) = \begin{Bmatrix} \dot{\mathbf{w}} \\ \mathbf{0} \\ \mathbf{0} \\ Q_{t-v} + \mathbf{e}_v^T \dot{\mathbf{w}} \end{Bmatrix}, \quad \begin{aligned} \rho &= \{\rho_1, \dots, \rho_{n_s}\}^T, & \dot{\mathbf{w}} &= \{\dot{w}_1, \dots, \dot{w}_{n_s}\}^T: \text{mass production rates per volume,} \\ \rho &= \sum_{s=1}^{n_s} \rho_s, & e_v &= \sum_{s=1}^{n_s} \frac{\rho_s}{\rho} e_{v_s}: \text{mixture vibrational energy per mass,} \\ p &= \sum_{s=1}^{n_s} \frac{\rho_s}{M_s} \bar{R} T, & \mathbf{e}_v &= \{e_{v_1}, \dots, e_{v_{n_s}}\}^T: \text{vibrational energies per mass,} \\ Q_{t-v} &: \text{translational-vibrational energy exchange,} \end{aligned}$$

$$E = \frac{|\mathbf{v}|^2}{2} + \sum_{s=1}^{n_s} \frac{\rho_s}{\rho} (c_V s T + e_{v_s} + h_s^o)$$

Vibrational Energy

Mixture vibrational energy per mass:

$$e_v = \sum_{s=1}^{n_s} \frac{\rho_s}{\rho} e_{v_s},$$

where

$$e_{v_s} = \begin{cases} \sum_{m=1}^{n_{v_s}} e_{v_{s,m}}(T_v) & \text{for molecules,} \\ 0 & \text{for atoms,} \end{cases}$$

and

$$e_{v_{s,m}}(T') = \frac{\bar{R}}{M_s} \frac{\theta_{v_{s,m}}}{\exp(\theta_{v_{s,m}}/T') - 1}$$

n_{v_s} : number of vibrational modes of species s ($n_{v_s} = 0$ for atoms)

$\theta_{v_{s,m}}$: characteristic vibrational temperature of mode m of species s

Translational–Vibrational Energy Exchange

Landau–Teller model:

$$Q_{t-v} = \sum_{s=1}^{n_s} \rho_s \sum_{m=1}^{n_{vs}} \frac{e_{vs,m}(T) - e_{vs,m}(T_v)}{\langle \tau_{s,m} \rangle}$$

Translational–vibrational energy relaxation time for mode m of species s :

$$\langle \tau_{s,m} \rangle = \left(\sum_{s'=1}^{n_s} \frac{y_{s'}}{\tau_{s,m,s'}} \right)^{-1} + \left[\left(N_A \sum_{s'=1}^{n_s} \frac{\rho_{s'}}{M_{s'}} \right) \sigma_{vs} \sqrt{\frac{8}{\pi} \frac{\bar{R}T}{M_s}} \right]^{-1},$$

where

$$y_s = \frac{\rho_s/M_s}{\sum_{s'=1}^{n_s} \rho_{s'}/M_{s'}}, \quad \tau_{s,m,s'} = \frac{\exp [a_{s,m,s'} (T^{-1/3} - b_{s,m,s'}) - 18.42]}{p'}, \quad \sigma_{vs} = \sigma'_{vs} \left(\frac{50,000 \text{ K}}{T} \right)^2$$

p' : pressure in atmospheres.

$a_{s,m,s'}$ and $b_{s,m,s'}$: vibrational constants for mode m of species s with colliding species s'

N_A : Avogadro constant

σ_{vs} : collision-limiting vibrational cross section

σ'_{vs} : collision-limiting vibrational cross section at 50,000 K.

Chemical Kinetics

Mass production rate per volume for species s :

$$\dot{w}_s = M_s \sum_{r=1}^{n_r} (\beta_{s,r} - \alpha_{s,r}) (R_{f_r} - R_{b_r})$$

Forward and backward reaction rates for reaction r :

$$R_{f_r} = \gamma k_{f_r} \prod_{s=1}^{n_s} \left(\frac{1}{\gamma} \frac{\rho_s}{M_s} \right)^{\alpha_{s,r}} \quad \text{and} \quad R_{b_r} = \gamma k_{b_r} \prod_{s=1}^{n_s} \left(\frac{1}{\gamma} \frac{\rho_s}{M_s} \right)^{\beta_{s,r}}$$

Forward and backward reaction rate coefficients:

$$k_{f_r}(T_c) = C_{f_r} T_c^{\eta_r} \exp(-\theta_r/T_c) \quad \text{and} \quad k_{b_r}(T) = \frac{k_{f_r}(T)}{K_{e_r}(T)}$$

Equilibrium constant for reaction r :

$$K_{e_r}(T) = \exp \left[A_{1_r} \left(\frac{T}{10,000 \text{ K}} \right) + A_{2_r} + A_{3_r} \ln \left(\frac{10,000 \text{ K}}{T} \right) + A_{4_r} \frac{10,000 \text{ K}}{T} + A_{5_r} \left(\frac{10,000 \text{ K}}{T} \right)^2 \right]$$

$\alpha_{s,r}$ and $\beta_{s,r}$: stoichiometric coefficients for species s in reaction r

γ : unit conversion factor

C_{f_r} , η_r , A_{i_r} : empirical parameters

θ_r : activation energy of reaction r , divided by Boltzmann constant

T_c : rate-controlling temperature ($T_c = \sqrt{T T_v}$ for dissociation, $T_c = T$ for exchange)

Scope of Code Verification

Conservation of mass, momentum, and energy:

$$\frac{\partial \mathbf{u}}{\partial t} + \nabla \cdot \mathbf{F}_c(\mathbf{u}) = -\nabla \cdot \mathbf{F}_p(\mathbf{u}) + \nabla \cdot \mathbf{F}_d(\mathbf{u}) + \mathbf{S}(\mathbf{u}),$$

where

$$\mathbf{u} = \begin{Bmatrix} \rho \\ \rho \mathbf{v} \\ \rho E \\ \rho e_v \end{Bmatrix}, \quad \mathbf{F}_c(\mathbf{u}) = \begin{Bmatrix} \rho \mathbf{v}^T \\ \rho \mathbf{v} \mathbf{v}^T \\ \rho E \mathbf{v}^T \\ \rho e_v \mathbf{v}^T \end{Bmatrix}, \quad \mathbf{F}_p(\mathbf{u}) = \begin{Bmatrix} \mathbf{0} \\ p \mathbf{I} \\ p \mathbf{v}^T \\ \mathbf{0}^T \end{Bmatrix}, \quad \mathbf{F}_d(\mathbf{u}) = \begin{Bmatrix} -\mathbf{J} \\ \boldsymbol{\tau} \\ (\boldsymbol{\tau} \mathbf{v} - \mathbf{q} - \mathbf{q}_v - \mathbf{J}^T \mathbf{h})^T \\ (-\mathbf{q}_v - \mathbf{J}^T \mathbf{e}_v)^T \end{Bmatrix},$$

$$\mathbf{S}(\mathbf{u}) = \begin{Bmatrix} \dot{\mathbf{w}} \\ \mathbf{0} \\ 0 \\ Q_{t-v} + \mathbf{e}_v^T \dot{\mathbf{w}} \end{Bmatrix}, \quad \begin{aligned} \boldsymbol{\rho} &= \{\rho_1, \dots, \rho_{n_s}\}^T, & \dot{\mathbf{w}} &= \{\dot{w}_1, \dots, \dot{w}_{n_s}\}^T: \text{mass production rates per volume,} \\ \rho &= \sum_{s=1}^{n_s} \rho_s, & e_v &= \sum_{s=1}^{n_s} \frac{\rho_s}{\rho} e_{v_s}: \text{mixture vibrational energy per mass,} \\ p &= \sum_{s=1}^{n_s} \frac{\rho_s}{M_s} \bar{R} T, & \mathbf{e}_v &= \{e_{v_1}, \dots, e_{v_{n_s}}\}^T: \text{vibrational energies per mass,} \\ Q_{t-v} &: \text{translational-vibrational energy exchange,} \end{aligned}$$

$$E = \frac{|\mathbf{v}|^2}{2} + \sum_{s=1}^{n_s} \frac{\rho_s}{\rho} (c_{v_s} T + e_{v_s} + h_s^o)$$

Scope of Code Verification

Conservation of mass, momentum, and energy:

Non-diffusive flux gradients

Thermochemical source term

$$\frac{\partial \mathbf{u}}{\partial t} + \nabla \cdot \mathbf{F}_c(\mathbf{u}) = -\nabla \cdot \mathbf{F}_p(\mathbf{u}) + \nabla \cdot \mathbf{F}_d(\mathbf{u}) + \mathbf{S}(\mathbf{u}),$$

where

$$\mathbf{u} = \begin{Bmatrix} \rho \\ \rho \mathbf{v} \\ \rho E \\ \rho e_v \end{Bmatrix}, \quad \mathbf{F}_c(\mathbf{u}) = \begin{Bmatrix} \rho \mathbf{v}^T \\ \rho \mathbf{v} \mathbf{v}^T \\ \rho E \mathbf{v}^T \\ \rho e_v \mathbf{v}^T \end{Bmatrix}, \quad \mathbf{F}_p(\mathbf{u}) = \begin{Bmatrix} \mathbf{0} \\ p \mathbf{I} \\ p \mathbf{v}^T \\ \mathbf{0}^T \end{Bmatrix}, \quad \mathbf{F}_d(\mathbf{u}) = \begin{Bmatrix} -\mathbf{J} \\ \tau \\ (\tau \mathbf{v} - \mathbf{q} - \mathbf{q}_v - \mathbf{J}^T \mathbf{h})^T \\ (-\mathbf{q}_v - \mathbf{J}^T \mathbf{e}_v)^T \end{Bmatrix},$$

$$\mathbf{S}(\mathbf{u}) = \begin{Bmatrix} \dot{\mathbf{w}} \\ \mathbf{0} \\ 0 \\ Q_{t-v} + \mathbf{e}_v^T \dot{\mathbf{w}} \end{Bmatrix}, \quad \begin{aligned} \rho &= \{\rho_1, \dots, \rho_{n_s}\}^T, & \dot{\mathbf{w}} &= \{\dot{w}_1, \dots, \dot{w}_{n_s}\}^T: \text{mass production rates per volume,} \\ \rho &= \sum_{s=1}^{n_s} \rho_s, & e_v &= \sum_{s=1}^{n_s} \frac{\rho_s}{\rho} e_{v_s}: \text{mixture vibrational energy per mass,} \\ p &= \sum_{s=1}^{n_s} \frac{\rho_s}{M_s} \bar{R} T, & \mathbf{e}_v &= \{e_{v_1}, \dots, e_{v_{n_s}}\}^T: \text{vibrational energies per mass,} \\ Q_{t-v} &: \text{translational-vibrational energy exchange,} \end{aligned}$$

$$E = \frac{|\mathbf{v}|^2}{2} + \sum_{s=1}^{n_s} \frac{\rho_s}{\rho} (c_V s T + e_{v_s} + h_s^o)$$

Scope of Code Verification

Conservation of mass, momentum, and energy:

Non-diffusive flux gradients

$$\frac{\partial \mathbf{u}}{\partial t} + \nabla \cdot \mathbf{F}_c(\mathbf{u}) = -\nabla \cdot \mathbf{F}_p(\mathbf{u}) + \nabla \cdot \mathbf{F}_d(\mathbf{u}) + \mathbf{S}(\mathbf{u}),$$

where

Spatial discretization

$$\mathbf{u} = \begin{Bmatrix} \rho \\ \rho \mathbf{v} \\ \rho E \\ \rho e_v \end{Bmatrix}, \quad \mathbf{F}_c(\mathbf{u}) = \begin{Bmatrix} \rho \mathbf{v}^T \\ \rho \mathbf{v} \mathbf{v}^T \\ \rho E \mathbf{v}^T \\ \rho e_v \mathbf{v}^T \end{Bmatrix}, \quad \mathbf{F}_p(\mathbf{u}) = \begin{Bmatrix} \mathbf{0} \\ p \mathbf{I} \\ p \mathbf{v}^T \\ \mathbf{0}^T \end{Bmatrix}, \quad \mathbf{F}_d(\mathbf{u}) = \begin{Bmatrix} -\mathbf{J} \\ \tau \\ (\tau \mathbf{v} - \mathbf{q} - \mathbf{q}_v - \mathbf{J}^T \mathbf{h})^T \\ (-\mathbf{q}_v - \mathbf{J}^T \mathbf{e}_v)^T \end{Bmatrix},$$

$$\mathbf{S}(\mathbf{u}) = \begin{Bmatrix} \dot{\mathbf{w}} \\ \mathbf{0} \\ 0 \\ Q_{t-v} + \mathbf{e}_v^T \dot{\mathbf{w}} \end{Bmatrix}, \quad \begin{aligned} \rho &= \{\rho_1, \dots, \rho_{n_s}\}^T, & \dot{\mathbf{w}} &= \{\dot{w}_1, \dots, \dot{w}_{n_s}\}^T: \text{mass production rates per volume,} \\ \rho &= \sum_{s=1}^{n_s} \rho_s, & e_v &= \sum_{s=1}^{n_s} \frac{\rho_s}{\rho} e_{v_s}: \text{mixture vibrational energy per mass,} \\ p &= \sum_{s=1}^{n_s} \frac{\rho_s}{M_s} \bar{R} T, & \mathbf{e}_v &= \{e_{v_1}, \dots, e_{v_{n_s}}\}^T: \text{vibrational energies per mass,} \\ Q_{t-v} &: \text{translational-vibrational energy exchange,} \end{aligned}$$

$$E = \frac{|\mathbf{v}|^2}{2} + \sum_{s=1}^{n_s} \frac{\rho_s}{\rho} (c_{V_s} T + e_{v_s} + h_s^o)$$

Scope of Code Verification

Conservation of mass, momentum, and energy:

Thermochemical source term

$$\frac{\partial \mathbf{u}}{\partial t} + \nabla \cdot \mathbf{F}_c(\mathbf{u}) = -\nabla \cdot \mathbf{F}_p(\mathbf{u}) + \nabla \cdot \mathbf{F}_d(\mathbf{u}) + \mathbf{S}(\mathbf{u}),$$

where

Implementation

$$\mathbf{u} = \begin{Bmatrix} \rho \\ \rho \mathbf{v} \\ \rho E \\ \rho e_v \end{Bmatrix}, \quad \mathbf{F}_c(\mathbf{u}) = \begin{Bmatrix} \rho \mathbf{v}^T \\ \rho \mathbf{v} \mathbf{v}^T \\ \rho E \mathbf{v}^T \\ \rho e_v \mathbf{v}^T \end{Bmatrix}, \quad \mathbf{F}_p(\mathbf{u}) = \begin{Bmatrix} \mathbf{0} \\ p \mathbf{I} \\ p \mathbf{v}^T \\ \mathbf{0}^T \end{Bmatrix}, \quad \mathbf{F}_d(\mathbf{u}) = \begin{Bmatrix} -\mathbf{J} \\ \tau \\ (\tau \mathbf{v} - \mathbf{q} - \mathbf{q}_v - \mathbf{J}^T \mathbf{h})^T \\ (-\mathbf{q}_v - \mathbf{J}^T \mathbf{e}_v)^T \end{Bmatrix},$$

$$\mathbf{S}(\mathbf{u}) = \begin{Bmatrix} \dot{\mathbf{w}} \\ \mathbf{0} \\ \mathbf{0} \\ Q_{t-v} + \mathbf{e}_v^T \dot{\mathbf{w}} \end{Bmatrix}, \quad \begin{aligned} \rho &= \{\rho_1, \dots, \rho_{n_s}\}^T, & \dot{\mathbf{w}} &= \{\dot{w}_1, \dots, \dot{w}_{n_s}\}^T: \text{mass production rates per volume,} \\ \rho &= \sum_{s=1}^{n_s} \rho_s, & e_v &= \sum_{s=1}^{n_s} \frac{\rho_s}{\rho} e_{v_s}: \text{mixture vibrational energy per mass,} \\ p &= \sum_{s=1}^{n_s} \frac{\rho_s}{M_s} \bar{R} T, & \mathbf{e}_v &= \{e_{v_1}, \dots, e_{v_{n_s}}\}^T: \text{vibrational energies per mass,} \\ Q_{t-v} &: \text{translational-vibrational energy exchange,} \end{aligned}$$

$$E = \frac{|\mathbf{v}|^2}{2} + \sum_{s=1}^{n_s} \frac{\rho_s}{\rho} (c_V s T + e_{v_s} + h_s^o)$$

1D Supersonic Flow using a Manufactured Solution

- One-dimensional domain: $x \in [0, 1]$ m
- Boundary conditions:
 - Supersonic inflow ($x = 0$ m)
 - Supersonic outflow ($x = 1$ m)
- 5 uniform meshes: 50, 100, 200, 400, 800 elements
- Solution consists of small, smooth perturbations to uniform flow:

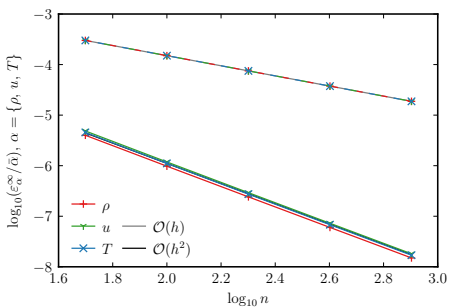
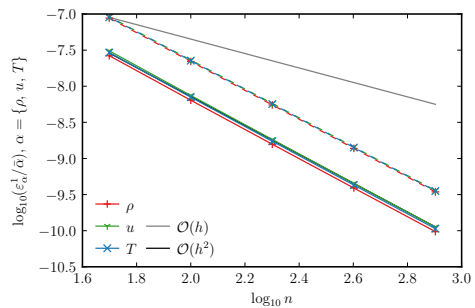
$$\rho(x) = \bar{\rho} [1 - \epsilon \sin(\pi x)],$$

$$u(x) = \bar{u} [1 - \epsilon \sin(\pi x)],$$

$$T(x) = \bar{T} [1 + \epsilon \sin(\pi x)],$$

$$\bar{\rho} = 1 \text{ kg/m}^3, \bar{T} = 300 \text{ K}, \bar{M} = 2.5, \epsilon = 0.05$$

1D Supersonic Flow using a Manufactured Solution



First-order accurate

Second-order accurate

Mesh	Original boundary conditions			Corrected boundary conditions		
	ρ	u	T	ρ	u	T
1–2	1.0008	1.0008	1.0008	2.0313	2.0362	2.0351
2–3	1.0002	1.0002	1.0002	2.0157	2.0184	2.0178
3–4	1.0001	1.0001	1.0000	2.0079	2.0093	2.0090
4–5	1.0000	1.0000	1.0000	2.0040	2.0047	2.0045

Observed accuracy p using L^∞ -norms of the error

2D Supersonic Flow using a Manufactured Solution

- Two-dimensional domain: $(x, y) \in [0, 1] \text{ m} \times [0, 1] \text{ m}$
- Boundary conditions:
 - Supersonic inflow ($x = 0 \text{ m}$)
 - Supersonic outflow ($x = 1 \text{ m}$)
 - Slip wall (tangent flow) ($y = 0 \text{ m}$ & $y = 1 \text{ m}$)
- 5 nonuniform meshes: $25 \times 25 \rightarrow 400 \times 400$
- Solution consists of small, smooth perturbations to uniform flow:

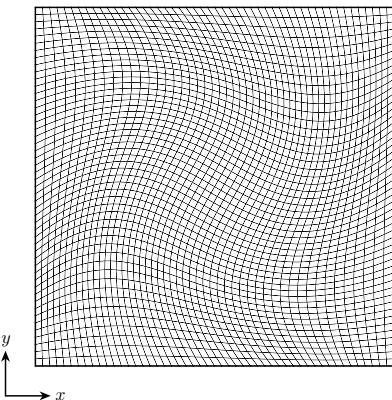
$$\rho(x, y) = \bar{\rho} [1 - \epsilon \sin(\frac{5}{4}\pi x) (\sin(\pi y) + \cos(\pi y))],$$

$$u(x, y) = \bar{u} [1 + \epsilon \sin(\frac{1}{4}\pi x) (\sin(\pi y) + \cos(\pi y))],$$

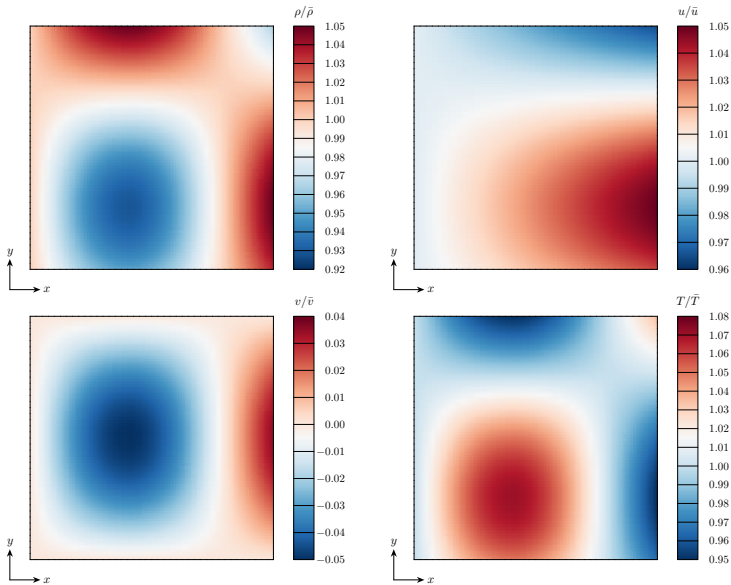
$$v(x, y) = \bar{v} [-\epsilon \sin(\frac{5}{4}\pi x) (\sin(\pi y) + \cos(\pi y))],$$

$$T(x, y) = \bar{T} [1 + \epsilon \sin(\frac{5}{4}\pi x) (\sin(\pi y) + \cos(\pi y))],$$

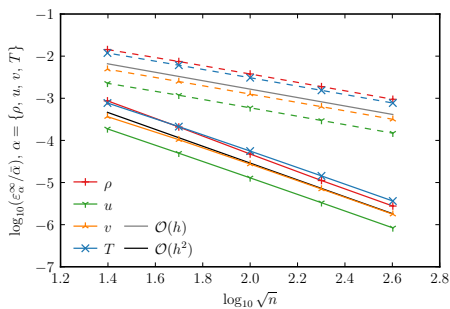
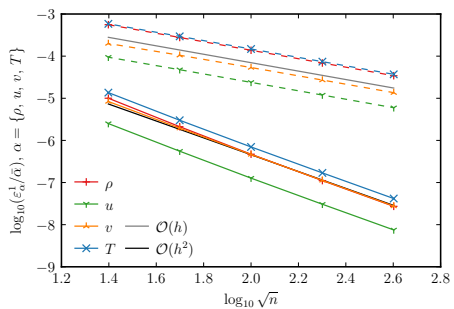
$$\bar{\rho} = 1 \text{ kg/m}^3, \bar{T} = 300 \text{ K}, \bar{M} = 2.5, \epsilon = 0.05$$



2D Supersonic Flow using a Manufactured Solution



2D Supersonic Flow using a Manufactured Solution



First-order accurate

Second-order accurate

Mesh	Original boundary conditions				Corrected boundary conditions			
	ρ	u	v	T	ρ	u	v	T
1–2	0.9420	0.9409	0.9721	0.9628	2.0623	1.9188	1.8174	1.8598
2–3	0.9850	0.9902	0.9910	0.9874	2.1304	1.9450	1.9221	1.9280
3–4	0.9960	1.0002	0.9924	0.9952	2.0902	1.9603	1.9671	1.9586
4–5	0.9989	1.0009	0.9959	0.9984	2.0128	1.9823	1.9860	1.9809

Observed accuracy p using L^{∞} -norms of the error

2D Supersonic Flow using an Exact Solution

- Two-dimensional domain: $(r, \theta) \in [1, 1.384] \times [0, 90]^\circ$
- Boundary conditions:
 - Supersonic inflow ($\theta = 90^\circ$)
 - Supersonic outflow ($\theta = 0^\circ$)
 - Slip wall (tangent flow) ($r = 1$ & $r = 1.384$)
- 6 meshes: $32 \times 8 \rightarrow 1024 \times 256$
- Solution is steady isentropic vortex:

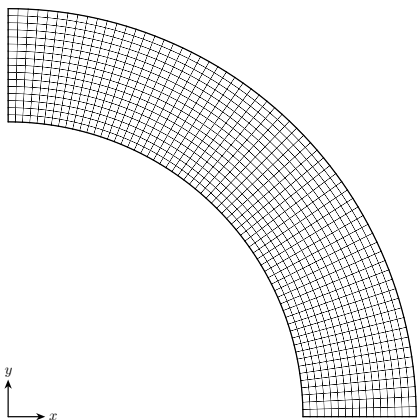
$$\rho(r) = \rho_i \left[1 + \frac{\gamma - 1}{2} M_i^2 \left(1 - \left(\frac{r_i}{r} \right)^2 \right) \right]^{\frac{1}{\gamma-1}},$$

$$u_r(r) = 0,$$

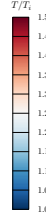
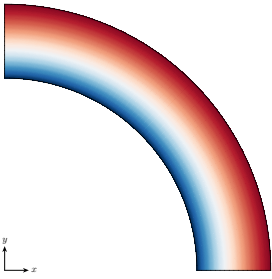
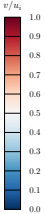
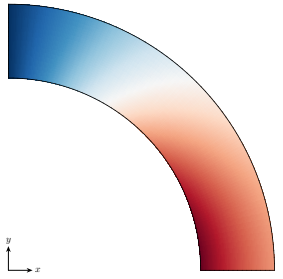
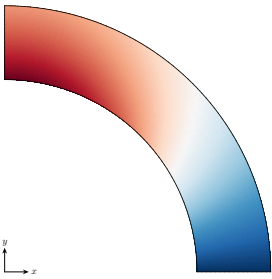
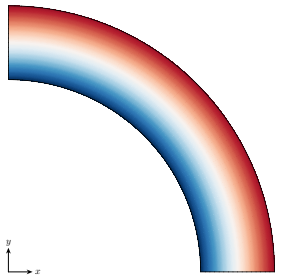
$$u_\theta(r) = -a_i M_i \frac{r_i}{r},$$

$$T(r) = T_i \left[1 + \frac{\gamma - 1}{2} M_i^2 \left(1 - \left(\frac{r_i}{r} \right)^2 \right) \right],$$

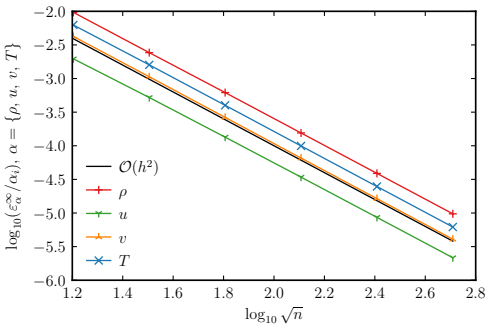
$$\rho_i = 1, a_i = 1, M_i = 2.25, T_i = 1/(\gamma R)$$



2D Supersonic Flow using an Exact Solution



2D Supersonic Flow using an Exact Solution



Mesh	ρ	u	v	T
1–2	1.9896	1.9119	1.9943	1.9699
2–3	1.9735	1.9589	2.0070	1.9979
3–4	1.9954	1.9760	2.0099	2.0076
4–5	1.9972	1.9879	2.0054	2.0044
5–6	1.9986	1.9940	2.0029	2.0025

Observed accuracy p using L^∞ -norms of the error

3D Supersonic Flow using a Manufactured Solution

- Three-dimensional domain: $(x, y, z) \in [0, 1] \text{ m} \times [0, 1] \text{ m} \times [0, 1] \text{ m}$
- Boundary conditions:
 - Supersonic inflow ($x = 0 \text{ m}$)
 - Supersonic outflow ($x = 1 \text{ m}$)
 - Slip wall (tangent flow)
($y = 0 \text{ m}, y = 1 \text{ m}, z = 0 \text{ m}, z = 1 \text{ m}$)

- 5 nonuniform meshes:
 $25 \times 25 \times 25 \rightarrow 400 \times 400 \times 400$

- Solution consists of small, smooth perturbations to uniform flow:

$$\rho(x, y, z) = \bar{\rho}[1 - \epsilon \sin(\frac{5}{4}\pi x)(\sin(\pi y) + \cos(\pi y))(\sin(\pi z) + \cos(\pi z))],$$

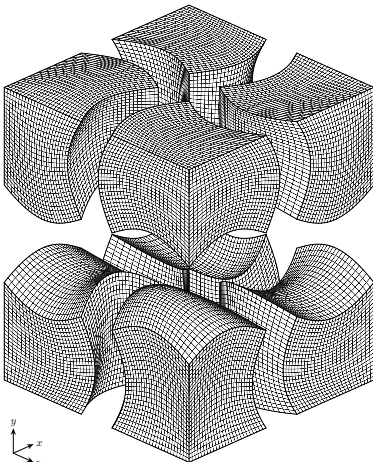
$$u(x, y, z) = \bar{u}[1 + \epsilon \sin(\frac{1}{4}\pi x)(\sin(\pi y) + \cos(\pi y))(\sin(\pi z) + \cos(\pi z))],$$

$$v(x, y, z) = \bar{v}[-\epsilon \sin(\frac{5}{4}\pi x)(\sin(\pi y) + \cos(\pi y))(\sin(\pi z) + \cos(\pi z))],$$

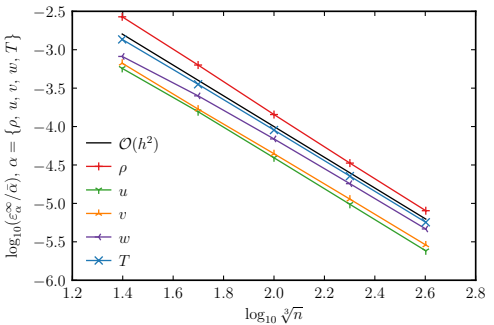
$$w(x, y, z) = \bar{w}[-\epsilon \sin(\frac{5}{4}\pi x)(\sin(\pi y) + \cos(\pi y))(\sin(\pi z) + \cos(\pi z))],$$

$$T(x, y, z) = \bar{T}[1 + \epsilon \sin(\frac{5}{4}\pi x)(\sin(\pi y) + \cos(\pi y))(\sin(\pi z) + \cos(\pi z))],$$

$$\bar{\rho} = 1 \text{ kg/m}^3, \bar{T} = 300 \text{ K}, \bar{M} = 2.5, \epsilon = 0.05$$



3D Supersonic Flow using a Manufactured Solution



Mesh	ρ	u	v	w	T
1–2	2.0849	1.8731	1.9841	1.7039	1.9404
2–3	2.1406	1.9923	1.9295	1.8621	1.9774
3–4	2.0990	2.0115	1.9623	1.9349	1.9922
4–5	2.0585	2.0100	1.9820	1.9571	1.9964

Observed accuracy p using L^∞ -norms of the error

Five-Species Air Model

5 species: N_2 , O_2 , NO , N , and O

17 reactions:

r	Reaction	Type of Reaction
1–5	$\text{N}_2 + \mathcal{M} \rightleftharpoons \text{N} + \text{N} + \mathcal{M}, \quad \mathcal{M} = \{\text{N}_2, \text{O}_2, \text{NO}, \text{N}, \text{O}\}$	Dissociation
6–10	$\text{O}_2 + \mathcal{M} \rightleftharpoons \text{O} + \text{O} + \mathcal{M}, \quad \mathcal{M} = \{\text{N}_2, \text{O}_2, \text{NO}, \text{N}, \text{O}\}$	Dissociation
11–15	$\text{NO} + \mathcal{M} \rightleftharpoons \text{N} + \text{O} + \mathcal{M}, \quad \mathcal{M} = \{\text{N}_2, \text{O}_2, \text{NO}, \text{N}, \text{O}\}$	Dissociation
16	$\text{N}_2 + \text{O} \rightleftharpoons \text{N} + \text{NO}$	Exchange
17	$\text{NO} + \text{O} \rightleftharpoons \text{N} + \text{O}_2$	Exchange

5-Species, 17-Reactions Inviscid Flow in Chemical Nonequilibrium

- Two-dimensional domain: $(x, y) \in [0, 1] \text{ m} \times [0, 1] \text{ m}$
- Same boundary conditions
- 7 nonuniform meshes: $25 \times 25 \rightarrow 1600 \times 1600$
- Solution consists of small, smooth perturbations to uniform flow

$$\rho_{\text{N}_2}(x, y) = \bar{\rho}_{\text{N}_2} [1 - \epsilon \sin(\frac{5}{4}\pi x) (\sin(\pi y) + \cos(\pi y))],$$

$$\rho_{\text{O}_2}(x, y) = \bar{\rho}_{\text{O}_2} [1 + \epsilon \sin(\frac{3}{4}\pi x) (\sin(\pi y) + \cos(\pi y))],$$

$$\rho_{\text{NO}}(x, y) = \bar{\rho}_{\text{NO}} [1 + \epsilon \sin(\pi x) (\sin(\pi y) + \cos(\pi y))],$$

$$\rho_{\text{N}}(x, y) = \bar{\rho}_{\text{N}} [1 + \epsilon \sin(\pi x) (\cos(\frac{1}{4}\pi y) + \sin(\frac{1}{4}\pi y))],$$

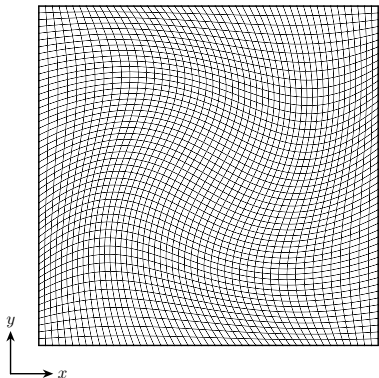
$$\rho_{\text{O}}(x, y) = \bar{\rho}_{\text{O}} [1 + \epsilon \sin(\pi x) (\sin(\pi y) + \cos(\frac{1}{4}\pi y))],$$

$$u(x, y) = \bar{u} [1 + \epsilon \sin(\frac{1}{4}\pi x) (\sin(\pi y) + \cos(\pi y))],$$

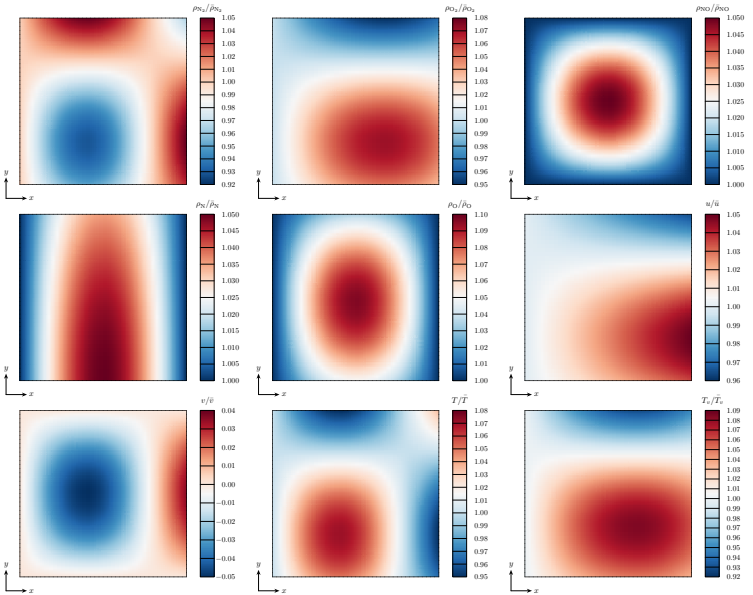
$$v(x, y) = \bar{v} [-\epsilon \sin(\frac{5}{4}\pi x) (\sin(\pi y) + \cos(\pi y))],$$

$$T(x, y) = \bar{T} [1 + \epsilon \sin(\frac{5}{4}\pi x) (\sin(\pi y) + \cos(\pi y))],$$

$$T_v(x, y) = \bar{T}_v [1 + \epsilon \sin(\frac{3}{4}\pi x) (\sin(\frac{5}{4}\pi y) + \cos(\frac{3}{4}\pi y))]$$

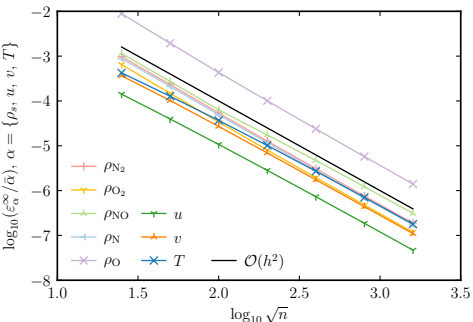


Five-Species Inviscid Flow in Chemical Nonequilibrium



2D Supersonic Flow in Thermal Equilibrium using a Manufactured Solution

Variable	Value	Units
$\bar{\rho}_{N_2}$	0.77	kg/m ³
$\bar{\rho}_{O_2}$	0.20	kg/m ³
$\bar{\rho}_{NO}$	0.01	kg/m ³
$\bar{\rho}_N$	0.01	kg/m ³
$\bar{\rho}_O$	0.01	kg/m ³
\bar{T}	3500	K
\bar{M}	2.5	
ϵ	0.05	

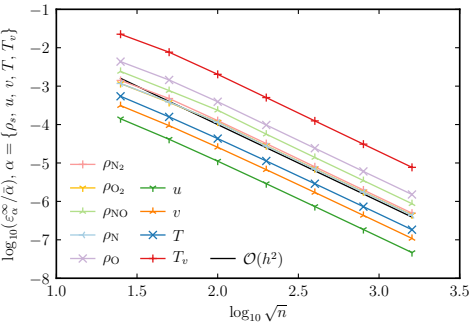


Mesh	ρ_{N_2}	ρ_{O_2}	ρ_{NO}	ρ_N	ρ_O	u	v	T
1–2	2.0608	2.1382	2.0698	2.0644	2.1885	1.8425	1.8289	1.7351
2–3	2.1161	2.1219	2.1127	2.1072	2.1697	1.8875	1.9220	1.7923
3–4	2.0798	2.0813	1.8555	2.0754	2.0971	1.9200	1.9686	1.8525
4–5	2.0456	2.0458	1.8917	2.0428	2.0806	1.9522	1.9871	1.9079
5–6	2.0243	2.0243	1.9427	2.0228	2.0529	1.9735	1.9939	1.9485
6–7	2.0125	2.0125	1.9790	2.0118	2.0318	1.9865	1.9969	1.9737

2D MMS, $n_s = 5$, $T_v = T$, $\dot{\mathbf{w}} \neq \mathbf{0}$: Observed accuracy p using L^∞ -norms of the error

2D Hypersonic Flow in Thermal Nonequilibrium using a Manufactured Solution

Variable	Value	Units
$\bar{\rho}_{N_2}$	0.0077	kg/m ³
$\bar{\rho}_{O_2}$	0.0020	kg/m ³
$\bar{\rho}_{NO}$	0.0001	kg/m ³
$\bar{\rho}_N$	0.0001	kg/m ³
$\bar{\rho}_O$	0.0001	kg/m ³
\bar{T}	5000	K
\bar{T}_v	1000	K
\bar{M}	8	
ϵ	0.05	



Mesh	ρ_{N_2}	ρ_{O_2}	ρ_{NO}	ρ_N	ρ_O	u	v	T	T_v
1–2	1.5659	1.6370	1.6555	1.6046	1.5869	1.7742	1.7337	1.7814	1.5545
2–3	1.9067	1.6944	1.6986	1.7598	1.8819	1.8916	1.8701	1.8768	1.9150
3–4	1.9868	2.0475	2.0698	2.0477	2.0110	1.9488	1.9357	1.9349	2.0082
4–5	2.0074	1.9941	2.0138	1.9936	2.0089	1.9752	1.9684	1.9672	2.0168
5–6	2.0062	1.9939	2.0004	1.9935	2.0061	1.9879	1.9843	1.9836	2.0111
6–7	2.0037	1.9965	1.9994	1.9962	1.9955	1.9940	1.9922	1.9918	2.0063

2D MMS, $n_s = 5$, $T_v \neq T$, $\dot{\mathbf{w}} \neq \mathbf{0}$: Observed accuracy p using L^∞ -norms of the error

Verification Techniques for Thermochemical Source Term

- $\mathbf{S}(\mathbf{u}) = [\dot{\mathbf{w}}; \mathbf{0}; 0; Q_{t-v} + \mathbf{e}_v^T \dot{\mathbf{w}}]$ is algebraic
 - $\mathbf{S}(\mathbf{u})$ computed by same code for both sides of $\mathbf{r}_h(\mathbf{u}_h) = \mathbf{r}(\mathbf{u}_{\text{MS}})$
 - Manufactured solutions will **not** detect implementation errors

Verification Techniques for Thermochemical Source Term

- $\mathbf{S}(\mathbf{u}) = [\dot{\mathbf{w}}; \mathbf{0}; 0; Q_{t-v} + \mathbf{e}_v^T \dot{\mathbf{w}}]$ is algebraic
 - $\mathbf{S}(\mathbf{u})$ computed by same code for both sides of $\mathbf{r}_h(\mathbf{u}_h) = \mathbf{r}(\mathbf{u}_{\text{MS}})$
 - Manufactured solutions will **not** detect implementation errors
- Compute $Q_{t-v}(\rho, T, T_v)$, $\mathbf{e}_v(\rho, T, T_v)$, and $\dot{\mathbf{w}}(\rho, T, T_v)$
 - For single-cell mesh when initialized to $\{\rho, T, T_v\}$ with no velocity
 - For many values of $\{\rho, T, T_v\}$
 - Compare with independently developed code
 - Perform convergence studies on distribution and difference

Verification Techniques for Thermochemical Source Term

- $\mathbf{S}(\mathbf{u}) = [\dot{\mathbf{w}}; \mathbf{0}; 0; Q_{t-v} + \mathbf{e}_v^T \dot{\mathbf{w}}]$ is algebraic
 - $\mathbf{S}(\mathbf{u})$ computed by same code for both sides of $\mathbf{r}_h(\mathbf{u}_h) = \mathbf{r}(\mathbf{u}_{\text{MS}})$
 - Manufactured solutions will **not** detect implementation errors
- Compute $Q_{t-v}(\rho, T, T_v)$, $\mathbf{e}_v(\rho, T, T_v)$, and $\dot{\mathbf{w}}(\rho, T, T_v)$
 - For single-cell mesh when initialized to $\{\rho, T, T_v\}$ with no velocity
 - For many values of $\{\rho, T, T_v\}$
 - Compare with independently developed code
 - Perform convergence studies on distribution and difference
- For each query, compute symmetric relative difference

$$\delta_\beta = 2 \frac{|\beta_{\text{SPARC}} - \beta'|}{|\beta_{\text{SPARC}}| + |\beta'|}$$

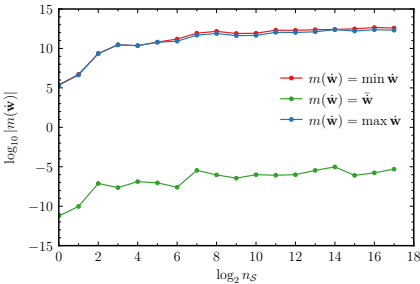
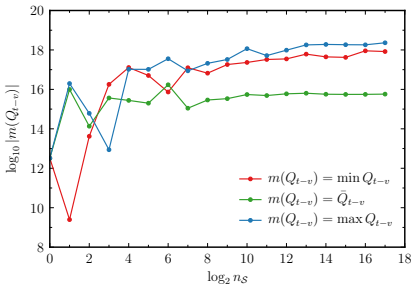
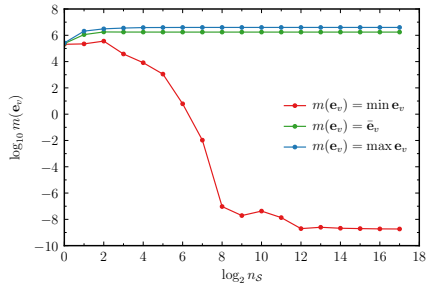
$$\beta = \left\{ Q_{t-v}, e_{v_{\text{N}_2}}, e_{v_{\text{O}_2}}, e_{v_{\text{NO}}}, \dot{w}_{\text{N}_2}, \dot{w}_{\text{O}_2}, \dot{w}_{\text{NO}}, \dot{w}_{\text{N}}, \dot{w}_{\text{O}} \right\}$$

Convergence History of $Q_{t-v}(\rho, T, T_v)$, $\mathbf{e}_v(\rho, T, T_v)$, and $\dot{\mathbf{w}}(\rho, T, T_v)$

Variable	Minimum	Maximum	Units	Spacing
ρ_{N_2}	10^{-6}	10^1	kg/m^3	Logarithmic
ρ_{O_2}	10^{-6}	10^1	kg/m^3	Logarithmic
ρ_{NO}	10^{-6}	10^1	kg/m^3	Logarithmic
ρ_{N}	10^{-6}	10^1	kg/m^3	Logarithmic
ρ_{O}	10^{-6}	10^1	kg/m^3	Logarithmic
T	100	15,000	K	Linear
T_v	100	15,000	K	Linear

Ranges and spacings for Latin hypercube samples

Minimum, mean, and maximum

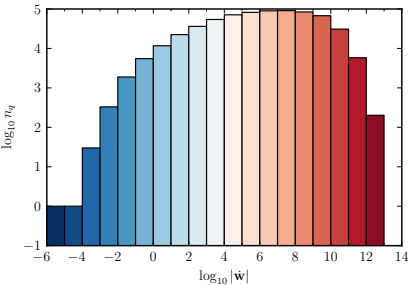
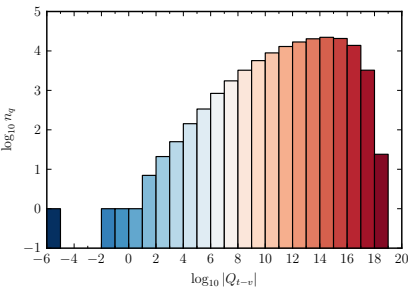
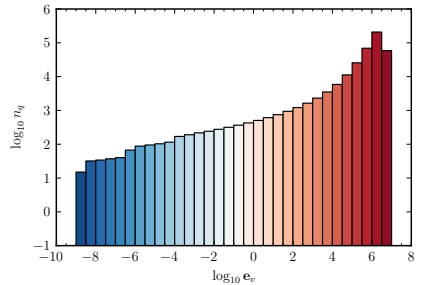


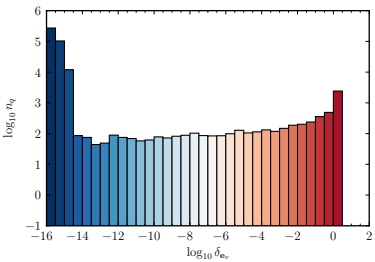
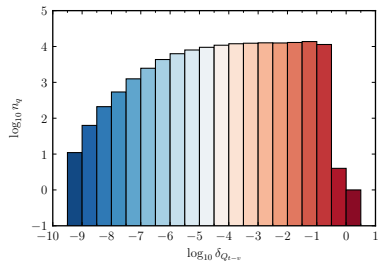
Distributions of $Q_{t-v}(\rho, T, T_v)$, $\mathbf{e}_v(\rho, T, T_v)$, and $\dot{\mathbf{w}}(\rho, T, T_v)$

Variable	Minimum	Maximum	Units	Spacing
ρ_{N_2}	10^{-6}	10^1	kg/m^3	Logarithmic
ρ_{O_2}	10^{-6}	10^1	kg/m^3	Logarithmic
ρ_{NO}	10^{-6}	10^1	kg/m^3	Logarithmic
ρ_{N}	10^{-6}	10^1	kg/m^3	Logarithmic
ρ_{O}	10^{-6}	10^1	kg/m^3	Logarithmic
T	100	15,000	K	Linear
T_v	100	15,000	K	Linear

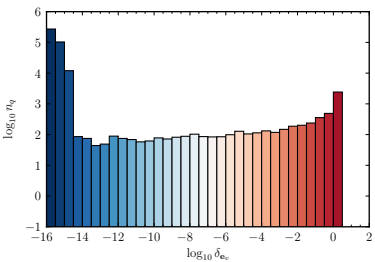
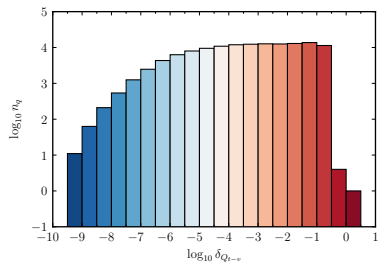
Ranges and spacings for Latin hypercube samples

Distribution of absolute values for $n_S = 2^{17} = 131,072$

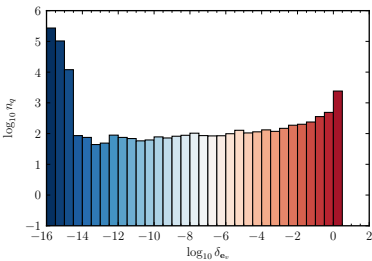
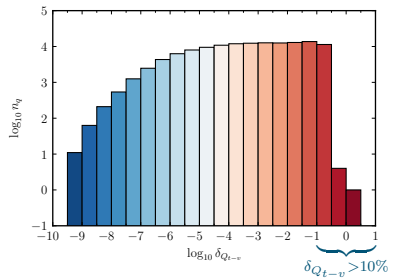


Original Nonzero Relative Differences in Q_{t-v} and \mathbf{e}_v 

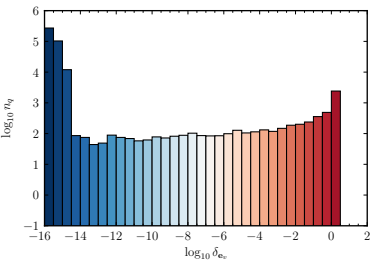
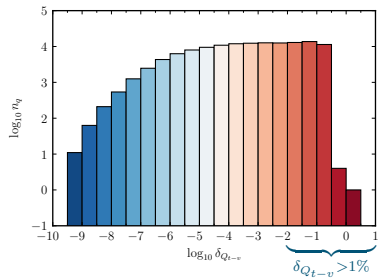
Original Nonzero Relative Differences in Q_{t-v} and \mathbf{e}_v



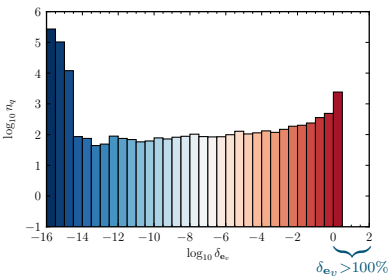
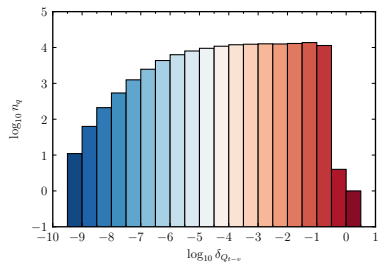
- Relative differences are **not** near machine precision

Original Nonzero Relative Differences in Q_{t-v} and \mathbf{e}_v 

- Relative differences are **not** near machine precision
- $\delta_{Q_{t-v}} > 10\%$ in 8.7% of simulations

Original Nonzero Relative Differences in Q_{t-v} and \mathbf{e}_v 

- Relative differences are **not** near machine precision
- $\delta_{Q_{t-v}} > 10\%$ in 8.7% of simulations
- $\delta_{Q_{t-v}} > 1\%$ in 29% of simulations

Original Nonzero Relative Differences in Q_{t-v} and \mathbf{e}_v 

- Relative differences are **not** near machine precision
- $\delta_{Q_{t-v}} > 10\%$ in 8.7% of simulations
- $\delta_{Q_{t-v}} > 1\%$ in 29% of simulations
- $\delta_{\mathbf{e}_v} > 100\%$ for some simulations

Causes of Large Relative Differences in Q_{t-v} and \mathbf{e}_v

Two causes:

Causes of Large Relative Differences in Q_{t-v} and \mathbf{e}_v

Two causes:

- **Incorrect lookup table values** for vibrational constants
 - Introduced error in Q_{t-v} for all simulations

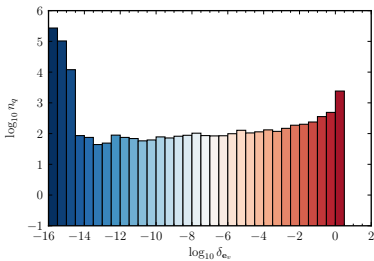
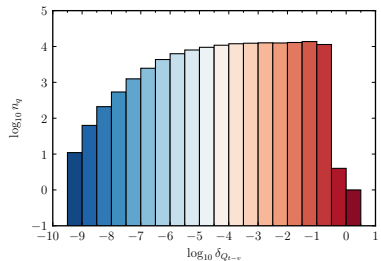
Causes of Large Relative Differences in Q_{t-v} and \mathbf{e}_v

Two causes:

- **Incorrect lookup table values** for vibrational constants
 - Introduced error in Q_{t-v} for all simulations
- **Loose convergence criteria** for computing T_v from $\rho \mathbf{e}_v$
 - Introduced errors in Q_{t-v} , \mathbf{e}_v , and $\dot{\mathbf{w}}$ for low values of T_v

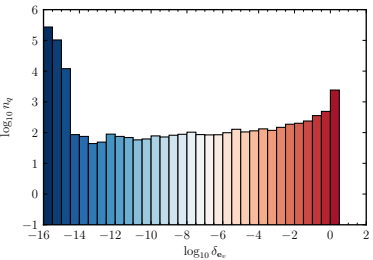
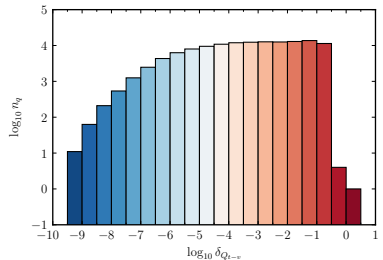
Corrected Nonzero Relative Differences in Q_{t-v} and \mathbf{e}_v

Original lookup table and convergence criteria

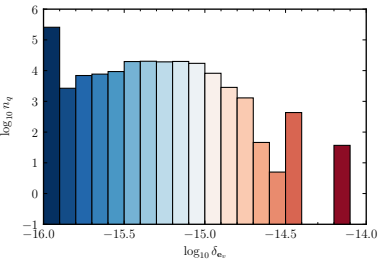
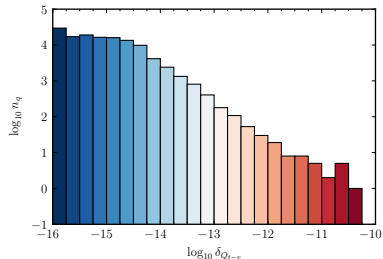


Corrected Nonzero Relative Differences in Q_{t-v} and \mathbf{e}_v

Original lookup table and convergence criteria

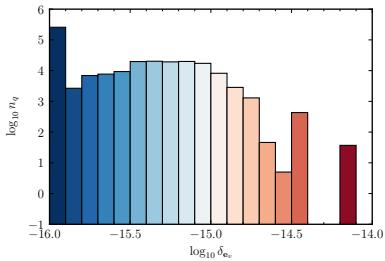
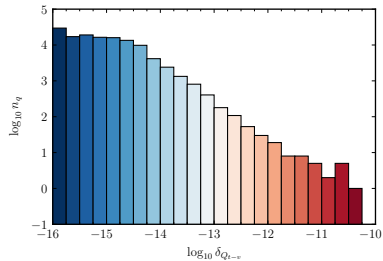


Corrected lookup table and tighter convergence criteria



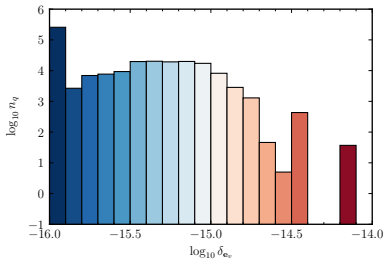
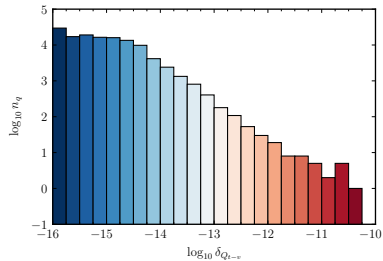
Corrected Nonzero Relative Differences in Q_{t-v} and \mathbf{e}_v

- Relative differences are consistent with our expectations



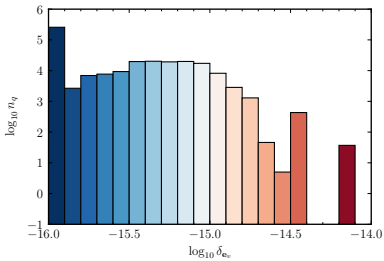
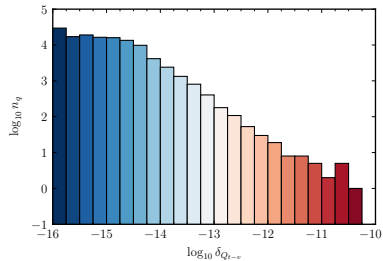
Corrected Nonzero Relative Differences in Q_{t-v} and \mathbf{e}_v

- Relative differences are consistent with our expectations
- $\delta_{Q_{t-v}} < 10^{-10}$ and $\delta_{\mathbf{e}_v} < 10^{-14}$ in all simulations



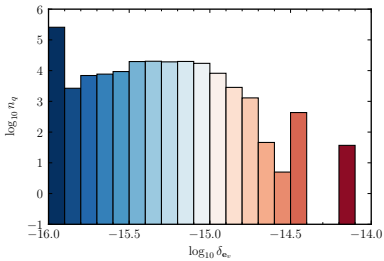
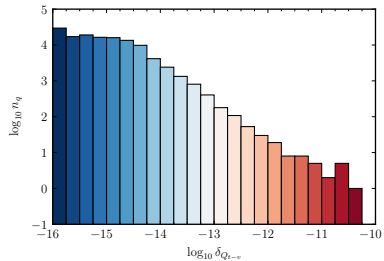
Corrected Nonzero Relative Differences in Q_{t-v} and \mathbf{e}_v

- Relative differences are consistent with our expectations
- $\delta_{Q_{t-v}} < 10^{-10}$ and $\delta_{\mathbf{e}_v} < 10^{-14}$ in all simulations
- $\delta_{Q_{t-v}} > 10^{-12}$ in 48/131,072 simulations



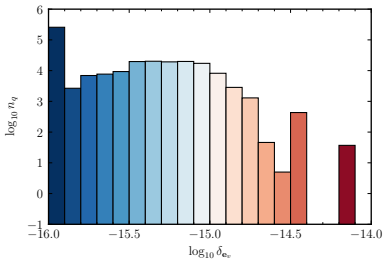
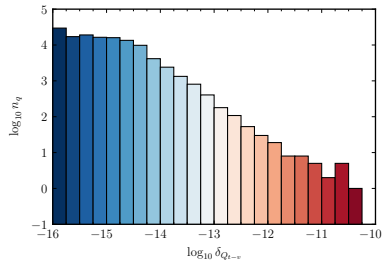
Corrected Nonzero Relative Differences in Q_{t-v} and \mathbf{e}_v

- Relative differences are consistent with our expectations
- $\delta_{Q_{t-v}} < 10^{-10}$ and $\delta_{\mathbf{e}_v} < 10^{-14}$ in all simulations
- $\delta_{Q_{t-v}} > 10^{-12}$ in 48/131,072 simulations
 - T and T_v have relative difference less than 0.2%



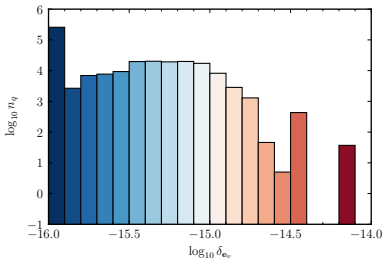
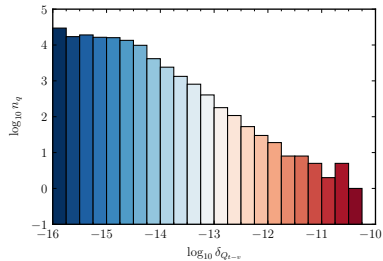
Corrected Nonzero Relative Differences in Q_{t-v} and \mathbf{e}_v

- Relative differences are consistent with our expectations
- $\delta_{Q_{t-v}} < 10^{-10}$ and $\delta_{\mathbf{e}_v} < 10^{-14}$ in all simulations
- $\delta_{Q_{t-v}} > 10^{-12}$ in 48/131,072 simulations
 - T and T_v have relative difference less than 0.2%
 - In numerator of $\frac{e_{v_{s,m}}(T) - e_{v_{s,m}}(T_v)}{\langle \tau_{s,m} \rangle}$, $e_{v_{s,m}}(T)$ and $e_{v_{s,m}}(T_v)$ share many leading digits



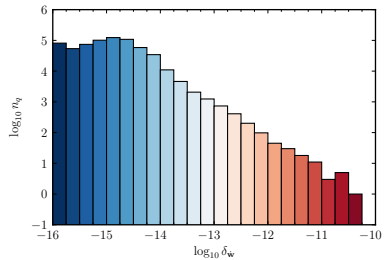
Corrected Nonzero Relative Differences in Q_{t-v} and \mathbf{e}_v

- Relative differences are consistent with our expectations
- $\delta_{Q_{t-v}} < 10^{-10}$ and $\delta_{\mathbf{e}_v} < 10^{-14}$ in all simulations
- $\delta_{Q_{t-v}} > 10^{-12}$ in 48/131,072 simulations
 - T and T_v have relative difference less than 0.2%
 - In numerator of $\frac{e_{v_{s,m}}(T) - e_{v_{s,m}}(T_v)}{\langle \tau_{s,m} \rangle}$, $e_{v_{s,m}}(T)$ and $e_{v_{s,m}}(T_v)$ share many leading digits
 - Precision lost when computing difference

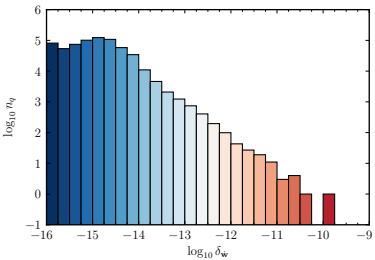


Nonzero Relative Differences in $\dot{\mathbf{w}}$

Original convergence criteria

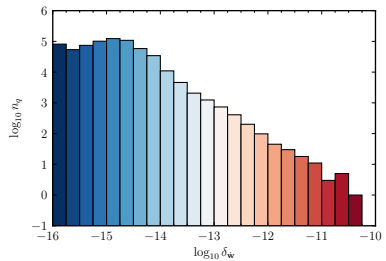


Tighter convergence criteria

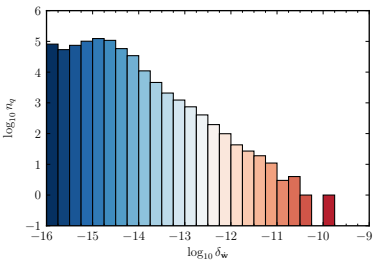


Nonzero Relative Differences in $\mathbf{\hat{w}}$

Original convergence criteria



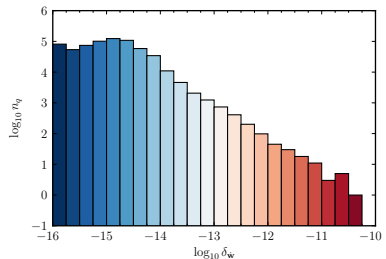
Tighter convergence criteria



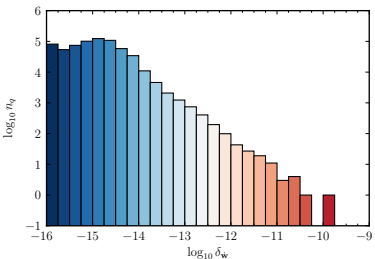
- Relative differences are consistent with our expectations

Nonzero Relative Differences in $\dot{\mathbf{w}}$

Original convergence criteria



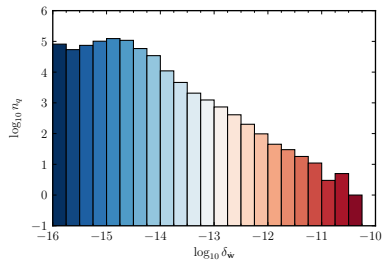
Tighter convergence criteria



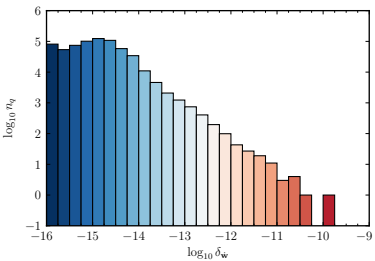
- Relative differences are consistent with our expectations
- $\delta_{\dot{\mathbf{w}}} < 10^{-9}$ in all simulations

Nonzero Relative Differences in $\dot{\mathbf{w}}$

Original convergence criteria



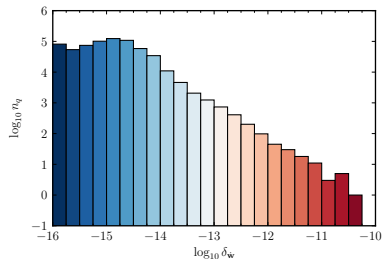
Tighter convergence criteria



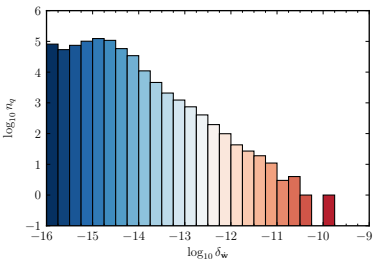
- Relative differences are consistent with our expectations
- $\delta_{\dot{\mathbf{w}}} < 10^{-9}$ in all simulations
- $\delta_{\dot{\mathbf{w}}} > 10^{-12}$ for 109/655,360 computed values (5 species, 131,072 simulations)

Nonzero Relative Differences in $\dot{\mathbf{w}}$

Original convergence criteria



Tighter convergence criteria



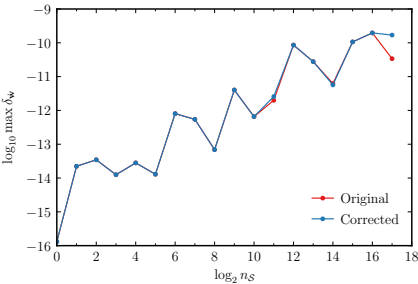
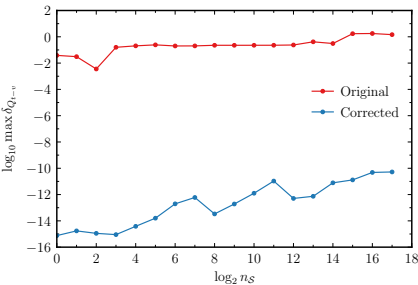
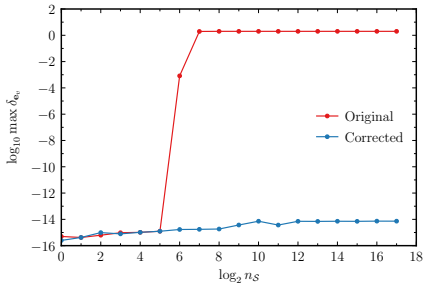
- Relative differences are consistent with our expectations
- $\delta_{\dot{\mathbf{w}}} < 10^{-9}$ in all simulations
- $\delta_{\dot{\mathbf{w}}} > 10^{-12}$ for 109/655,360 computed values (5 species, 131,072 simulations)
 - Due to precision loss that can occur from subtraction in
$$\dot{w}_s = M_s \sum_{r=1}^{n_r} (\beta_{s,r} - \alpha_{s,r}) (R_{f_r} - R_{b_r})$$

Maximum Differences in $Q_{t-v}(\rho, T, T_v)$, $\mathbf{e}_v(\rho, T, T_v)$, and $\dot{\mathbf{w}}(\rho, T, T_v)$

Variable	Minimum	Maximum	Units	Spacing
ρ_{N_2}	10^{-6}	10^1	kg/m^3	Logarithmic
ρ_{O_2}	10^{-6}	10^1	kg/m^3	Logarithmic
ρ_{NO}	10^{-6}	10^1	kg/m^3	Logarithmic
ρ_{N}	10^{-6}	10^1	kg/m^3	Logarithmic
ρ_{O}	10^{-6}	10^1	kg/m^3	Logarithmic
T	100	15,000	K	Linear
T_v	100	15,000	K	Linear

Ranges and spacings for Latin hypercube samples

Maximum relative differences



Summary

- Code verification plays important role in establishing simulation credibility
- Manufactured solutions are effective for verifying discretizations
 - Exercise features of interest
 - Effectively identify issues
 - Insufficient for algebraic source terms – both evaluations the same
- Many independent comparisons for algebraic terms
 - Effective approach for verifying implementation – detected multiple issues
 - Convergence study important to assess sample representation

Additional Information

- B. Freno, K. Carlberg

Machine-learning error models for approximate solutions
to parameterized systems of nonlinear equations

Computer Methods in Applied Mechanics and Engineering (2019)
[arXiv:1808.02097](https://arxiv.org/abs/1808.02097)

- B. Freno, B. Carnes, V. Weirs

Code-Verification techniques for hypersonic reacting flows
in thermochemical nonequilibrium

Journal of Computational Physics (2021)
[arXiv:2007.14376](https://arxiv.org/abs/2007.14376)

